Nano Today 26 (2019) 149–163

Contents lists available at ScienceDirect

Nano Today

journal homepage: www.elsevier.com/locate/nanotoday

Review

Fluorescent silicon nanomaterials: from synthesis to functionalization and application

Bin Song, Yao He*

Laboratory of Nanoscale Biochemical Analysis, Jiangsu Key Laboratory for Carbon-Based Functional Materials and Devices, Institute of Functional Nano & Soft Materials (FUNSOM) and Collaborative Innovation Center of Suzhou Nano Science and Technology (NANO-CIC), Soochow University, Suzhou, 215123, China

ARTICLE INFO

Article history:
Received 31 December 2018
Received in revised form 6 March 2019
Accepted 18 March 2019
Available online 28 March 2019

Keywords:
Silicon nanomaterials
Fluorescence
Synthesis
Functionalization

ABSTRACT

In the last decade, we have witnessed the giant achievement in the field of silicon materials. Among of them, fluorescent silicon nanomaterials have attracted considerable attentions owing to their unique advantages, including strong fluorescence coupled with robust photostability, rich resource support, low cost, industrial maturity, and good biocompatibility. Extensive efforts are devoted to developing effective methods for the synthesis and functionalization of fluorescent silicon nanomaterials with different nanostructures, facilitating the promotion of this promising material for myriad optical applications. In this review article, we systematically summarize representative progresses for the design and synthesis of fluorescent silicon nanomaterials during the last decade. We also present an in-depth description of functionalization strategies toward fluorescent silicon nanomaterials, with a particular focus on organic ligands-modification, doping and biological species-modification methods. Furthermore, typical optical applications (e.g., bioimaging, sensing, anti-counterfeiting and anti-bacterial applications) are introduced based on latest research achievements. Finally, future trends and current challenges are highlighted as a roadmap proposal for research in this field.

Contents

Introduction

Silicon is the second most abundant element in earth's crust, supporting a low-cost and rich resource for various silicon-based applications [1–3]. For over half a century, silicon has dominated the microelectronics industry. Being a typical kind of indirect-band gap semiconductor, bulk silicon displays poor photoluminescent properties at room temperature, thus limiting its optical applications [4–7]. Notably, novel structural and surface-dependent optical properties emerge when the size of silicon decreases to nanoscale. The quantum confinement effect and surface functionalization (The influence of surface state is also important at nanoscale, owing to the exciton Bohr radius of silicon is only ~4.2 nm.) process allow efficient fluorescence (photoluminescence quantum yield

* Corresponding author.
E-mail address: yaohe@suda.edu.cn (Y. He).

https://doi.org/10.1016/j.nantod.2019.03.005
1748-0132/

(PLQY) maximumly up to ~90%) from silicon nanomaterials [8–10]. Recently, taking advantages of their excellent optoelectronic properties, their various applications have reached the fields from physics to biomedicine [12–16]. To meet the increasing demand of silicon materials-based applications, fluorescent silicon nanomaterials with various structures have been developed, among which zero-dimensional fluorescent silicon nanoparticles (SiNPs), and one-dimensional fluorescent silicon nanorods (SiNRs) are in particular interest [17,18].

Today, numerous methods have been reported for preparing fluorescent silicon nanmaterials, principally involving in "top-down" or "bottom-up" procedures [12,17–19]. In addition, for acquiring desired optical properties and other functions, the investigation of silicon nanomaterials with reasonable surface architectures and functional dopants has gained great attentions. Consequently, these surface modification and doping strategies endow silicon nanomaterials with special multi-functionalities [12,14]. Despite tremendous achievements, a number of challenges remain as follow. The first crucial challenge is how to large-scale synthesize high-quality silicon nanomaterials in facile and practical manner. These practices need the materials to be prepared through relatively simple process with convincing mechanism. Another challenge is how to rationally functionalize the silicon nanosystems for special optical applications.

In this review article, we summarize the recent progress in synthesis, functionalization and optical applications of these zero- and one-dimensional fluorescent silicon nanomaterials. In the following section, we introduce the approaches for synthesizing zero-dimensional silicon nanoparticles (SiNPs) and one-dimensional silicon nanorods (SiNRs), and categorize representative synthesis strategies. In the next section, we review the recent works related to modifying silicon nanomaterials surfaces with organic ligands to improve their photoluminescence quantum yields (PLQY) and manipulate their emission wavelength. In addition, the progress of multi-functional silicon nanomaterials those combine with various types of dopants and biological functional species has also been systemically reviewed. Based on the great advances in the synthesis and functionalization of high-quality fluorescent silicon nanomaterials, we further conclude their related applications in a broad range of fields, including as fluorescence probes for sensing, as contrast agents for bioimaging, as multi-responsive materials for anti-counterfeiting applications. In the final section, the perspectives and challenges for the synthesis and application of fluorescent silicon nanomaterials in the future are discussed.

Design and synthesis

The fast development of fluorescent silicon nanomaterials with functional structures has greatly promoted the evolution of nanotechnology. The SiNPs and SiNRs are the typical zero-dimensional and one-dimensional silicon nanomaterials. In the last decades, researchers have made tremendous dedication in establishing a great deal of strategies to synthesize fluorescent silicon nanomatrials, which has been elaborately described in a number of previously reported papers [5–19]. In this section, we focus on summarizing representative progresses of synthesis of fluorescence SiNPs and SiNRs achieved during the last ten years.

Zero-dimensional fluorescent silicon nanoparticles

Within the past decade, numerous methods to prepare SiNPs have been developed, including electrochemical/chemical etching, high-temperature processes, solution-phase reduction, laser pyrolysis, microemulsion, plasma assisted aerosol precipitation, mechanochemical synthesis and microwave synthesis [20–30]. These approaches could be classified as "top-down" (Scheme 1 (a)) and "bottom-up" approaches (Scheme 1 (b)). One of the most important "top-down" methods for synthesizing fluorescent SiNPs is via decomposition of bulk silicon and silicon rich oxides. Sailor et al. reported this strategy with the mixture of hydrogen fluoride and H_2O_2 to etch porous silicon under the assist of ultrasound in electrochemical method, producing SiNPs with controlled wavelength of emission [31]. Kang and coworkers demonstrated a variant of the etching method where the color of fluorescence could be tunable from blue fluorescence to red scale as determined by the diameters of SiNPs [20]. For improving the pH stability and aqueous dispersibility of the resultant SiNPs, He et al. reported a UV-induced polymerization method to prepare polymer-coated water-dispersible silicon nanospheres (Fig. 1a) containing about tens to hundreds of nanoparticles with robust pH stability [28]. For synthesizing water-dispersible, small-sized and fluorescent SiNPs in rapid and facile way, in 2011, the same group developed a one-pot method for preparing SiNPs (Fig. 1b) using silicon nanowires and glutaric acid as the reaction precursors under microwave irradiation. Notably, the SiNPs display excellent pH-stability, aqueous dispersibility and small size (~4 nm) [29].

Besides, another approach to realize the "top-down" process is reduction of silicon oxides. Usually, the SiNPs could be annealed within SiO_x matrix, which produced from the silicon sub-oxide in precursors [32,33]. The approach was firstly demonstrated by Liu et al. where SiNPs (Fig. 1c) were prepared by etching the oxide layer from SiO_x powder after thermal anneal [34,35]. Comparatively, Veinot and coworkers produced silicon oxides as thin films through thermal decomposition of hydrogen silsesquioxane (HSQ). The fluorescent SiNPs with tunable emission wavelength could be obtained through an established HF etching method [36,37]. In 2012, Korgel et al. extended the thermal decomposition of HSQ method to synthesize SiNPs. The method relied on the high temperature (from 1100 to 1400 °C) reduction of HSQ to obtain SiNPs (Fig. 2d). The prepared SiNPs featured narrow size distribution, tunable size (from less than 3 nm up to 90 nm) and good crystallinity. Subsequent HF etching and thermal hydrosilylation with alkenes yielded fluorescent SiNPs (from visible to near-infrared emission) in organic solvent [38].

The alternative to the "top-down" methods introduced above to synthesize fluorescent SiNPs is through assembly of silicon-based small moleculars, so-called bottom-up approaches. One of the most popular "bottom-up" method is reducing silane in solution. The strategy was initially developed by Heath, who showed that the mixture of $SiCl_4$ and octyltrichlorosilane could produce polydispersed SiNPs under high temperature and pressure [39]. To assist with optimizing nanoparticle size distribution, Wilcoxon et al found that addition of surfactant molecules to the precursor to produce inverse micelle environment could further improve the size distribution [40]. Typically, in 2010, Tilley and coworkers reported chemical reactions on molecules (such as epoxides and diols) modified on the surface of SiNPs that could be performed to prepare SiNPs with special surface functionalities (Fig. 1e) [24]. A second class of strategies for the "bottom-up" synthesis of SiNPs involves in the utilization of silicon Zintl salts (ASi_x, A = K, Mg, Na etc.). Typically, the silicon Zintl salt was reacted with bromine gas and silicon halides. For example, Kauzlarich and coworkers synthesized SiNPs through the reaction between potassium silicide (KSi) and $SiCl_4$ in diglyme or glyme solution [21,41–44].

In particular, most of the above-introduced SiNPs generally possess poor water dispersibility, relatively tedious procedures, low yield, and severe reaction condition. In 2013, He and coworkers reported a rapid "bottom-up" microwave reaction for synthesizing blue-emission SiNPs with excellent aqueous dispersibility. Organic molecules (i.e., 3-(aminopropyl) trimethoxysilane, $C_6H_{17}NO_3Si$,

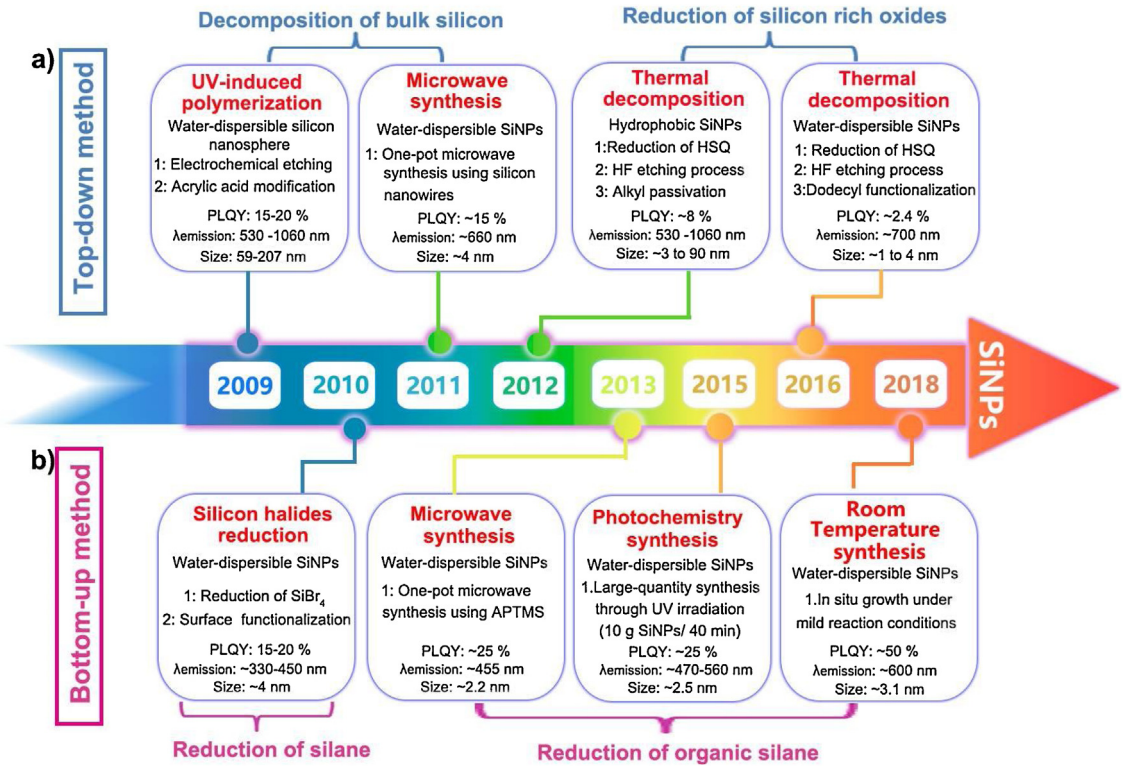

Scheme 1. (a, b) Illustration of typical synthetic strategies of fluorescent SiNPs during the last decade (2009–2018).

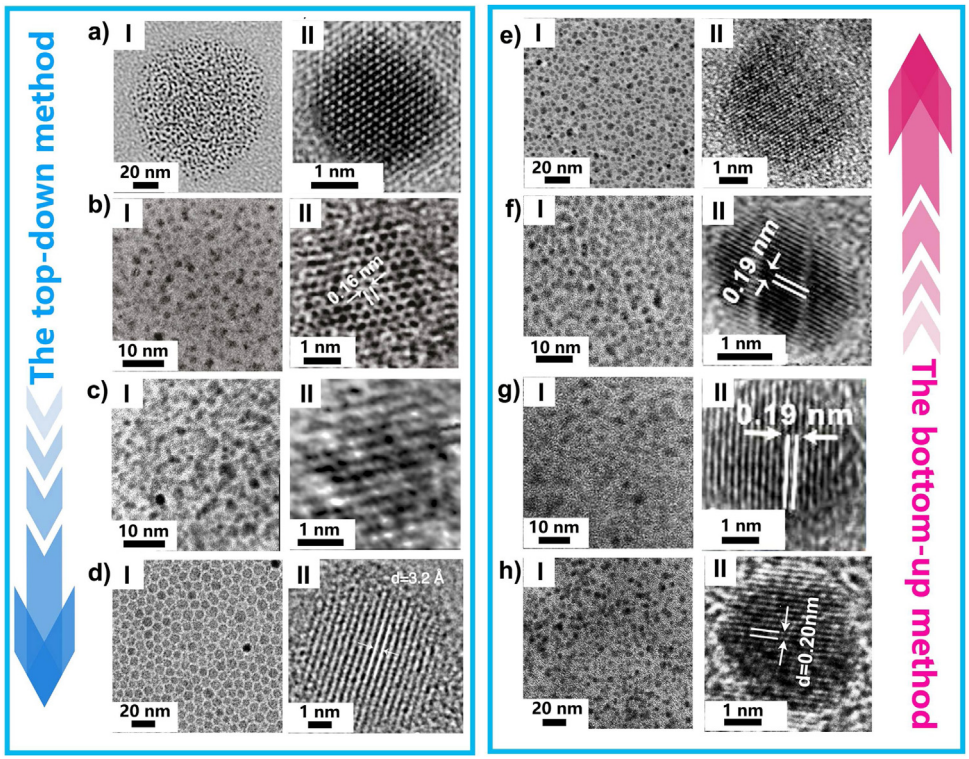

Fig. 1. TEM and HRTEM images of fluorescent SiNPs produced by the "top-down" (a–d) and "bottom-up" (e–h) methods. (a) Printed with permission from Wiley Publications [28]; (b) Printed with permission from ACS Publications [29]; (c) Printed with permission from ACS Publications [34]; (d) Printed with permission from ACS Publications [38]; (e) Printed with permission from ACS Publications [24]; (f) Printed with permission from ACS Publications [30]; (g) Printed with permission from ACS Publications [46]; (h) Printed with permission from RSC Publications [47].

(APTMS)), served as silicon-based reaction precursor, could be readily reduced to form SiNPs with highly fluorescent (PLQY: ~20%) and ultra-small (diameter: ~2.2 nm) via in situ growth through microwave irradiation. Significantly, in this system, merely ~10 min was required for the synthesis of ~0.1 g SiNPs (Fig. 1f) [30]. In addition, large-scale preparation of fluorescent SiNPs is the

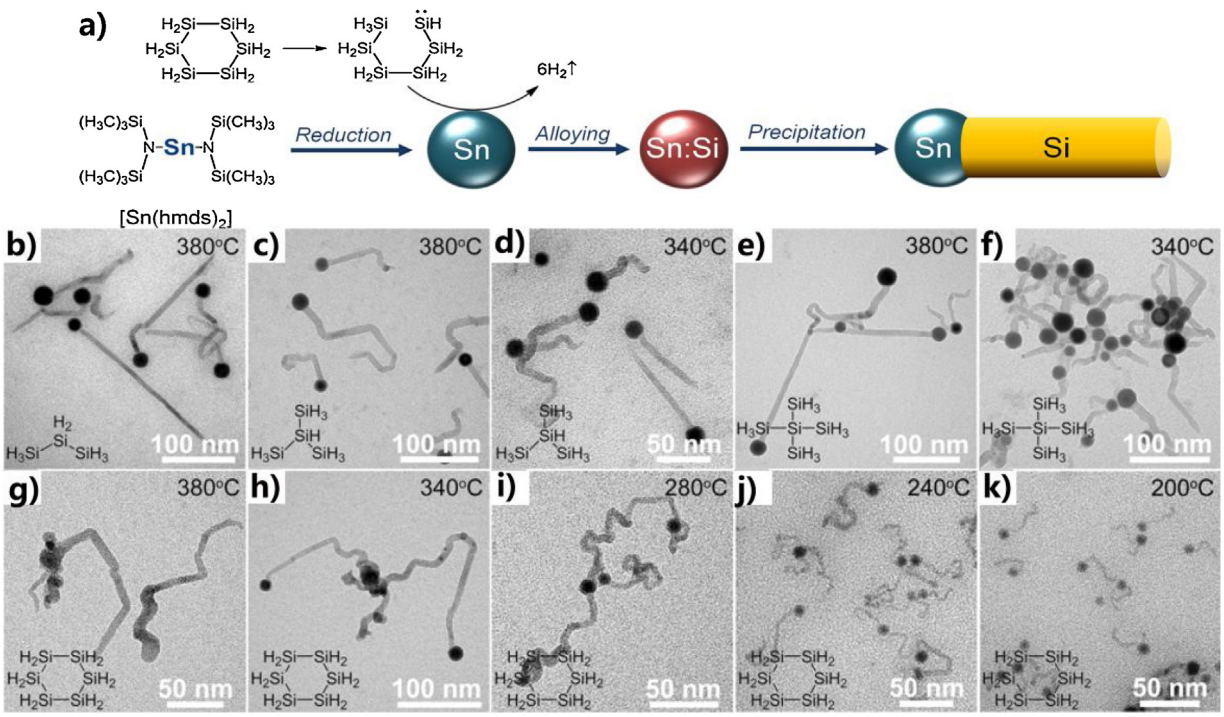

Fig. 2. (a) Illustration of SiNRs preparation using cyclohexasilane as precursor. Step 1: Sn $(hmds)_2$ was reduced in Sn nanoparticles. Step 2: the resultant Sn nanoparticles catalyzed the decomposition of silane producing hydrogen. The silicon dissolved in the Sn/Si alloy. Step 3: silicon precipitated on the surface of Sn/Si alloy and recrystallized into the SiNRs. (b–k) TEM images of SiNRs prepared from Sn-seeded solution liquid-solid method at various temperatures using different kinds of silane precursors: (b) trisilane at 380 °C; isotetrasilane at (c) 380 °C and (d) 340 °C; neopentasilane at (e) 380 °C and (f) 340 °C; cyclohexasilane at (g) 380 °C, (h) 340 °C, (i) 280 °C, (j) 240 °C, and (k) 200 °C. (a–k) Printed with permission from ACS Publications [65].

major premise for the wide-ranging optical application. Recently, Zhong et al. developed a photochemical method for synthesizing SiNPs with controllable optical properties. This strategy was capable of preparing large quality of SiNPs (ca. ~10 g) with tunable emission wavelength through a short reaction time (Fig. 1g). In this system, SiNPs with excellent photo- and pH-stability were obtained through reacting the mixture of the silicon precursor of 1,8-naphthalimide and APTMS under 365 nm irradiation. Finally, ~10 g of SiNPs with blue, green, and light-green emission could be prepared through 15, 30, and 40 min photochemical reaction time [45].

In spite of the exciting progresses in the synthesis of fluorescent SiNPs, toxic, flammable, expensive silicon resources or other reagents (e.g., glutaric acid, nitric acid/hydrofluoric etc.) were usually necessary as precursors, which generally impeded the simple availability of SiNPs and further lead to potential environmental pollution. In 2015, taking advantage of the attractive properties (e.g., silica framework, quasi-periodic mechanical structure and photonic crystal property etc.) of diatoms, a novel biomimetic method for preparing fluorescent, aqueous-dispersible SiNPs was demonstrated by Wu et al [46]. The red-emitting SiNPs were obtained from the diatom through microwave irradiation. Notably, the SiNPs (Fig. 2g) feature an ultra-narrow full-width-at half-maximum of ~30 nm, which is the lowest result in hydrophilic fluorescent SiNPs. For synthesizing fluorescent SiNPs in a facile way, Zhong et al. demonstrated that fluorescent SiNPs (diameter: ~3.1 nm) could be in situ growth quickly (~60 min) under facile and mild reaction conditions (i.e., atmospheric pressure and room temperature). In particular, the entire reaction could be readily realized in a common kind of glass bottle, without the requirement of any additional reaction instruments (Fig. 1h). Moreover, the resultant SiNPs featured strong fluorescence (PLQY: ~50%), robust photostability and favorable biocompatibility [47].

One-dimensional fluorescent silicon nanorods

One-dimensional (or pseudo-one-dimensional) fluorescent SiNRs are a special class of silicon nanostructures. The interesting and unique optical properties they exhibit have made them a powerful platform for the development of numerous kinds of probes and devices over the past decade [48–52]. For example, radiative electron-hole recombination rates and other photophysical process like Auger recombination can be significantly different in nanorods compared to nanoparticles. The one-dimenional nanostructure can lower thresholds for multiexction generation (the multiexciton yield in nanorods was about twice as high as in nanoparticles) and optical gain, which are important for high-efficacy devices and nanolaser [53–58]. Synthetic advances to achieve high-quality SiNRs with control over sizes, compositions and optical properties have further driven progress toward applications [59–66].

In 2009, Korgel and co-workers experimentally presented a class of one-dimensional silicon nanorods (SiNRs). In their reports, SiNRs with diameters as ~5 nm and lengths as ~75 nm could be prepared through a ligand-assisted solution liquid-solid (SLS) growth process. Gold crystals were utilized as seeds with decomposition of trisilane (Si_3H_8) as precursor. Dodecylamine was used as a functional ligand and was important to the growth process. The SiNRs length could be tuned from ~5 to ~75 nm by controlling the molar ratio of Si/Au, reaction temperature and solvent in the reaction [60]. Recently, the same group further developed a kind of fluorescent SiNRs. The fluorescent SiNRs with PLQY of 4–5% were synthesized by the Si_3H_8 in hot squalane (reaction temperature: 410 °C) with the presence of tin nanoparticles and dodecylamine, and followed by hydrofluoric acid-etching and thermal hydrosilylation [63]. In 2015, for improving the reaction efficiency and decreasing the reaction temperature, Prof. Korgel and collaborators demonstrated that polysilane hydrides (such as isotetrasilane, neopentasilane and cyclohexasilane) could be used to realize lower

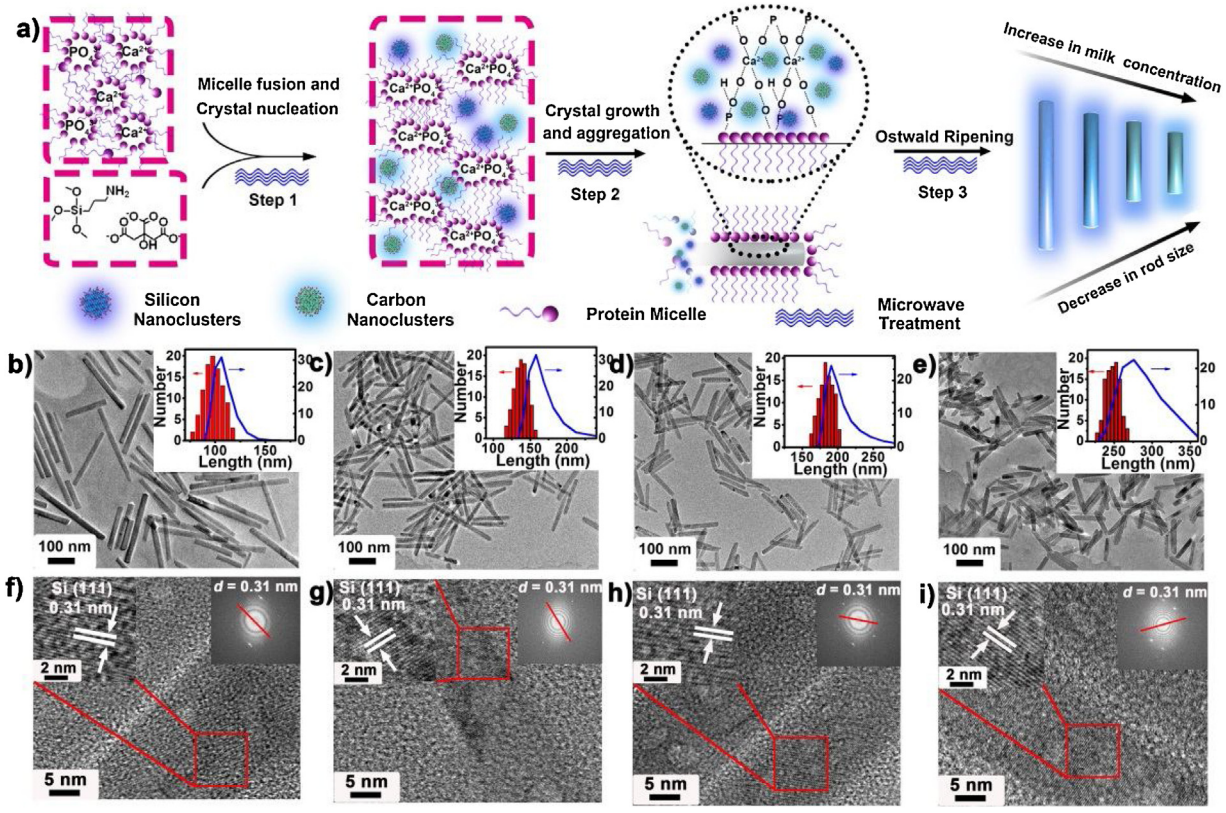

Fig. 3. (a) Schematic diagram of the preparation of SiNRs through microwave irradiation. The reaction process of SiNRs was composed of three steps. Step 1: crystal nucleation and micelle fusion. Step 2: crystal growth and oriented aggregation. Step 3: growth in longitudinal direction. (b–i) TEM characterizations of SiNRs with different sizes: (b, f) 250 nm; (c, g) 180 nm; (d, h) 140 nm; and (e, i) 100 nm. Insets in (b–e) show corresponding size distribution histogram and DLS analysis. (a–i) Printed with permission from ACS Publications [66].

reaction temperature than other silane molecules (Fig. 2). Among of them, cyclohexasilane allowed the lowest reaction temperature of ~200 °C, using a one-step SLS growth reaction from Sn seeds. Moreover, observed photoluminescence (QY of ~2%) could be achieved from SiNRs grown at low temperatures. Despite of these progresses of designing fluorescent SiNRs, it is still in high demand to develop a new kind of method to prepare high-quality fluorescent SiNRs [65]. In 2016, Song et al. developed a novel kind of SiNR with highly fluorescent, robust photostability and tunable lengths (~100–250 nm), could be readily synthesized through one-pot microwave reaction under facile and mild reaction conditions (e.g., reaction temperature: 150 °C; reaction time:60 min). In brief, silicon and carbon nanoclusters could be created in crystal nucleation stage through microwave reaction. Moreover, calcium phosphate crystallization was formed through typical fusion-fission effect between calcium and phosphorus ions linked protein micelles in the presence of silane, which improved the aggregation of the carbon and silicon nanoclusters, thus producing rod-like one-dimensional silicon nanostructure (Fig. 3). Of note, the resultant SiNRs featured excitation wavelength-dependent fluorescence property (emission wavelengths: from ~450 to 600 nm; the corresponding excitation wavelengths: from ~390 to 560 nm), and have been demonstrated for the fabrication of white-light-emitting devices (LEDs) [66].

Functionalization and application

Organic ligands-modified fluorescent silicon nanomaterials

Taking advantage of facile surface tailorability with well-developed silicon technology, silicon nanomaterials are enabling functionalized with special ligands [14]. These surface modification strategies allow for the synthesis of silicon nanomaterials with special functionalities and unique optical properties for various applications [15,18]. Relatively poor fluorescence performance of silicon nanomaterials remains great challenges due to the intrinsic indirect-band gap. PLQY, as the important quantified factor for the fluorescence property, is recognized as a significant description for evaluating whether a fluorescent material is suitable for wide-ranging optical applications [12]. In the last decade, researchers have made great contributions on the improvement of PLQY to obtain brighter fluorescent from silicon nanomaterials. More recently, organic ligands-modification has been developed as a significant method to improve the optical properties. Significantly, the influence of the ligands on the silicon nanomaterials' fluorescence have been comprehensively reported, which demonstrated that the structure and function of the surface ligands were critical for the ultra-bright fluorescence and tunable emission wavelength.

Representatively, Qian et al. bonded fluoro-substituted alkenes onto SiNPs surface through microwave irradiation to increase the PLQY of SiNPs in a facile and "green" manner. They indicated that the increased PLQY could be attributed to the minimization of non-radiative relaxation pathways, which induced by the low frequency of carbon-fluorine bond stretching. In addition, they also demonstrated that compared to those modified with dodecyl, functionalized SiNPs with perfluorodecyl have enhanced PL stability when exposure to moisture. The similar study from Qian et al. also demonstrated that adding heteroatoms (i.e., C–F or C–S) into the surface-bonded aryl or alkyl moieties would induce improved PLQY, due to the associated lowering of the C–X bond vibration frequency [67,68].

In 2013, Li, Shao and co-workers introduced a simple surface modification. In briefly, ultra-bright cyan-green fluorescence SiNPs

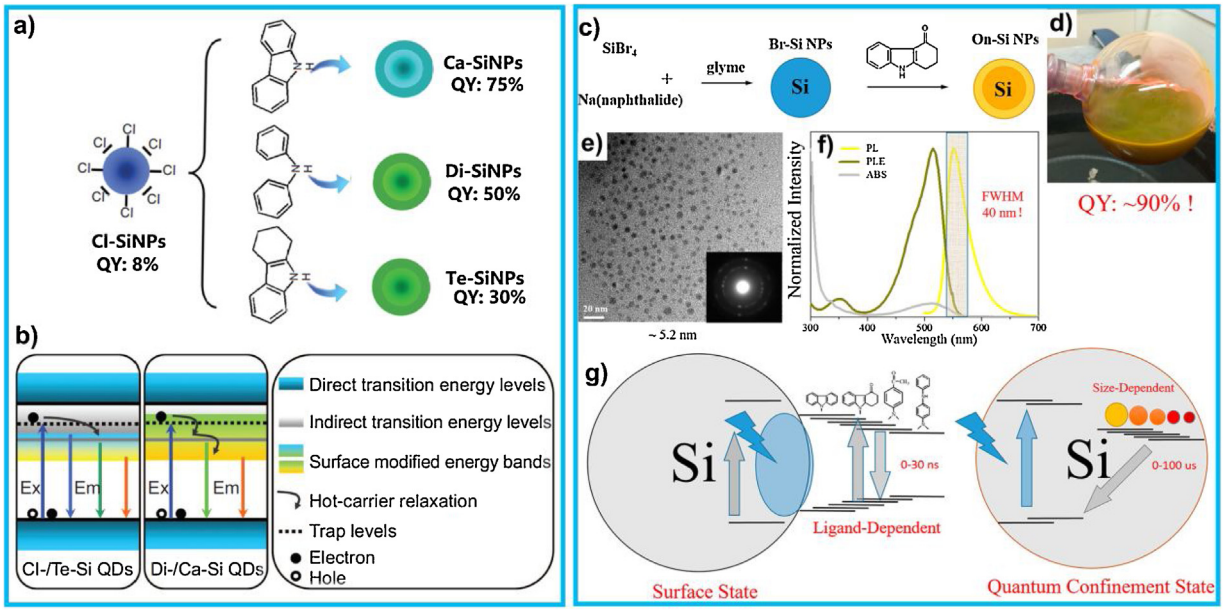

Fig. 4. (a) Illustration of ligands-modified SiNPs with enhanced PLQYs. (b) Illustration of the energy level arrangement for the two kinds of ligands-modified SiNPs. (c) Scheme of the synthesis and surface modification process to make yellow fluorescent SiNPs with high PLQY and small emission bandwidth. (d) Photograph of the as-prepared SiNPs (e) TEM image of SiNPs with an average size of ~5.2 nm. Inset is the selected-area electron diffraction pattern of the SiNPs. (f) Optical characterizations of the SiNPs. The PL bandwidth was very narrow (~40 nm). (g) Illustration of the surface PL from ligands-modified SiNPs and quantum confinement PL. (a, b) Printed with permission from Nature Publications [70]. (c–g) Printed with permission from ACS Publications [71].

with PLQYs up to 75% could be readily obtained through surface modification. A highly fluorescent recombination channel across the nanoparticles ensemble could be induced by the surface modification. According to the aromatic electron-rich system with high nucleophilicity of the chosen organic ligands (such as diphenylamine and carbazole, nitrogencontaining), the PL properties of SiNPs have been successfully modulated through this surface reaction [69].

In following study, they further interrogated the relationship between surface organic ligand modifications and energy band structures of SiNPs. Through systemically investigating the excited-state dynamics in different kinds of nitrogen element-containing ligands modified SiNPs (Fig. 4a), the PL mechanisms were unraveled through two kinds of interaction methods for surface-passivated SiNPs: 'weak' interaction and 'strong' interaction, depending on the influence of organic ligands on the excited-state channels (the interaction strength from the core and ligands) in SiNPs. Therefore, fabricating the organic molecular structure of capping ligands to enhance the density of state on the surface of SiNPs (i.e., the surface ligands with more phenyl rings) might effectively improve the PLQY of SiNPs (Fig. 4b) [70]. In 2016, the same authors reported surface nitrogen-capped yellow-emitting SiNPs with PLQY up to ~90% and narrow full-width-at half-maximum value of ~40 nm. The resultant SiNPs have a radiative decay with minimum nonradiative species, due to the favorable optical properties (Fig. 4c-g) [71]. The fluorescence mechanism operating in surface-modified SiNPs and the factors would affect their PL wavelength still need further investigation. In addition, Sailor et al. reported that the optical properties of SiNPs were highly surface-sensitive and related to the solvent polarity of environment. The dipole moment dependent emission has been interpreted as the stabilization of surface traps by alignment of molecular dipoles on the silicon surface [72,73]. In 2018, Peteanu et al. demonsreated that the high PLQY emission was arisen from a charge-transfer (CT) state between the silicon surface and organic ligands. The energy of the CT state was linearly dependent on the ground-state dipole moment of the ligands. In this study, the PL energy of SiNPs capped with special organic ligands could be quantitatively calculated from the ground state dipole moment of the surface organic ligands. Enhancing the polarity of the surface ligand would lead to a red-shift in the PL wavelength. As the ligands were strong electron donors, CT usually occurs from the ligand to the surface of SiNPs [74].

It is worthwhile to point out that, for biomedical application, the SiNPs need to be dispersible in water phase [12–15], in which an important barrier for the obtaining of high PLQY could be contributed by the dielectric screening effect due to the Coulomb interactions between SiNPs and water [75]. To address these issues, more recently, Shen, Song, and co-workers presented a general and facile method, i.e., solvent polarity-induced PL enhancement (SPIPE), which could enable several-fold enhancement in PLQY of SiNPs. In brief, three kinds of 4-substituented-1,8-naphthalic anhydride molecules were rationally prepared, which served as surface organic ligands for the synthesis of organic molecules-capped small-diameter (size: from 3.8 to 5.8 nm) SiNPs with PLQY of ~8%, ~15% and ~16%, respectively. Significantly, PLQY of the as-prepared SiNPs would be greatly increased from ~10% to ~50% through the SPIPE approach. According to the theoretical calculation, they revealed that the active excited-state CT interactions between surface coating and surface-covered organic ligand would be responsible for the prominent PLQY enhancement (Fig. 5a) [76]. Very recently, in 2018, Zhong et al. developed a new kind of approach for synthesis SiNPs with high PLQY. The reaction procedure could be rapidly (~1 h) programed through one-pot microwave irradiation, without the additional ligands for surface modification. In brief, the silicon source (APTMS) was first hydrolyzed to form hydration APTMS and then reduced by sodium fluorescein molecules to produce green-emitting SiNPs with ultra-high PLQY (~90%) [77].

It is worthwhile to note that, recent reports have revealed that surface ligand containing nitrogen element (e.g., N—H group) attached to SiNPs may play significant factors to control the emission wavelength of SiNPs. Recently, He's group demonstrated that obvious excitation-wavelength-dependent emission spectra

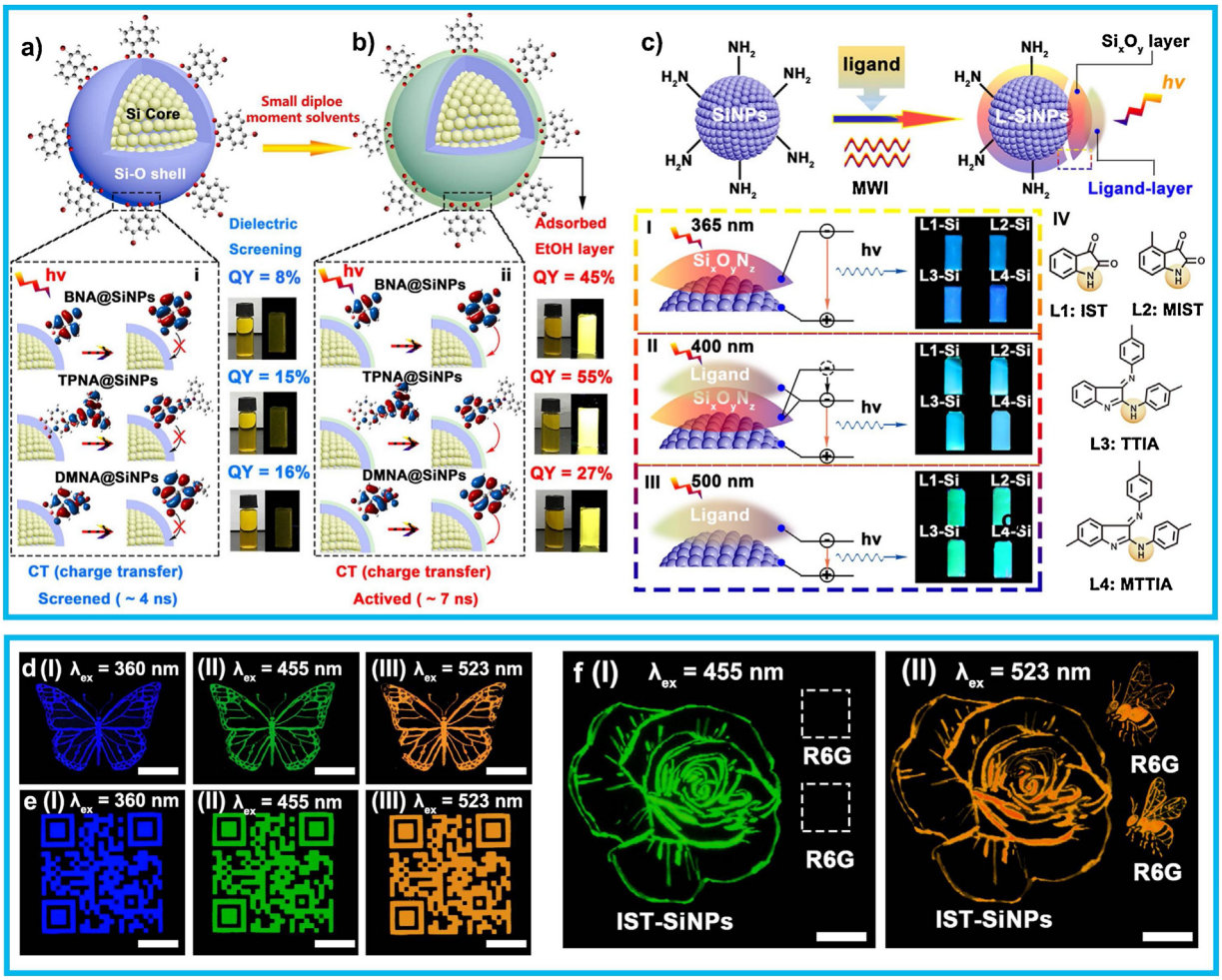

Fig. 5. (a, b) Mechanism illustration of SPIPE of SiNPs on the molecular level. (a) Schematic ligand-capped SiNP; (b) SiNP after treatment of small diploe moment solvents on surface; (a (i)) CT screened state; (b (ii)) CT active state. The ligands' electron density was calculated through DFT to show the CT process on the molecular level. (c) Illustration of preparation of ligands-modified SiNPs. (c (I–III)) Dashed line frame diaplayed the mechanism for excitation-wavelength-dependent PL of the SiNPs: the photons yielded from the process of exciton radiative recombination in various of gap states through different excitation wavelengths, leading to the excitation wavelength-dependent PL of SiNPs. (c (IV)) Molecular structures of the as-prepared oxidized indole ligands. Fluorescent photographs of commercially available papers stained with SiNPs ink. (d) Butterfly-patterned photographs imaged with excitation at: (I) 360 nm, (II) 455 nm, and (III) 523 nm. (e) Quick response -patterned photographs imaged with excitation at: (I) 360 nm, (II) 455 nm, and (III) 523 nm. (f) Rose- and bees-patterned photographs fabricated by SiNP- and R6 G-inks imaged with excitation at: (I) 455 nm, (II) 523 nm. Scale bar: 1 cm. (a,b) Printed with permission from Springer Publications [76]; (c–f) Printed with permission from RSC Publications [78].

of SiNPs could be readily prepared through modifying a new kind of organic ligands, i.e., oxidized indole derivatives (Fig. 5c). In this study, a crystalline silicon core with a SiO_xN_y-shell decorated by ligand was thus formed in the microwave reaction. They also demonstrated that the excitation-wavelength-dependent emission property (emission wavelengths ranged from ~420 to 550 nm, corresponding to excitation wavelengths ranged from ~350 to 520 nm) was ascribed to the formation of different kinds CT states at the Si/SiO_xN_y interface. In addition, they further exploited the as-prepared SiNPs as a new kind of optical label for multi-color anti-counterfeiting applications in different patterns [78]. On the other hand, recent studies showed that surface modificantion could offer a possibility of creating SiNPs with high PLQY and tunable fluorescence emission wavelength [79–84]. Veinot's group reported the prepared SiNPs with an average size of ~3-4 nm and surface modified with functional groups (i.e., dodecylamine, acetal, diphenylamine, TOPO and dodecyl) for realizing the tunable emission wavelength across the visible spectrum (from 450 nm to 720 nm). The origin of fluorescence from these functionalized SiNPs could be tentatively attributed to surface ligands mediated CT processes based on the excited-state lifetimes and solvatochromic studies [79].

Doped silicon fluorescent nanomaterials

To meet the increasing demands from various fields, doped silicon nanomaterials that combine silicon-based materials with other types of functional elements or nanostructures have recently gained great attentions. Recently, fluorescent silicon nanomaterials made of SiNPs doped with nonmetal or transition-metal have been well fabricated and utilized for bioimaging, biological/chemical sensors, disease diagnosis, catalysts, and solar cells etc [12–19,85–106]. For example, doping SiNPs with phosphorous (n-dopant) or boron (p-dopant) would enable the formation of p-n junctions [91–96]. In addition, doping of SiNPs with metal dopants in particular has been relatively unexplored. Kauzlarich et al. developed a multi-step process to prepare Mn- and Fe- doped SiNPs using metal-doped alkali silicides. Fe- and Mn-doped SiNPs demonstrated PL and paramagnetism properties, making them suitable candidates for multimodal bioimaging [97–99]. In 2015, Tilley developed a generalized approach to dope SiNPs with different kinds of transition metals (Cu, Ni and Mn), through the reduction of halide salts method. Such doped SiNPs featured excellent fluorescent properties including emission red shifts of over 40 nm and increased subgap absorption. [102].

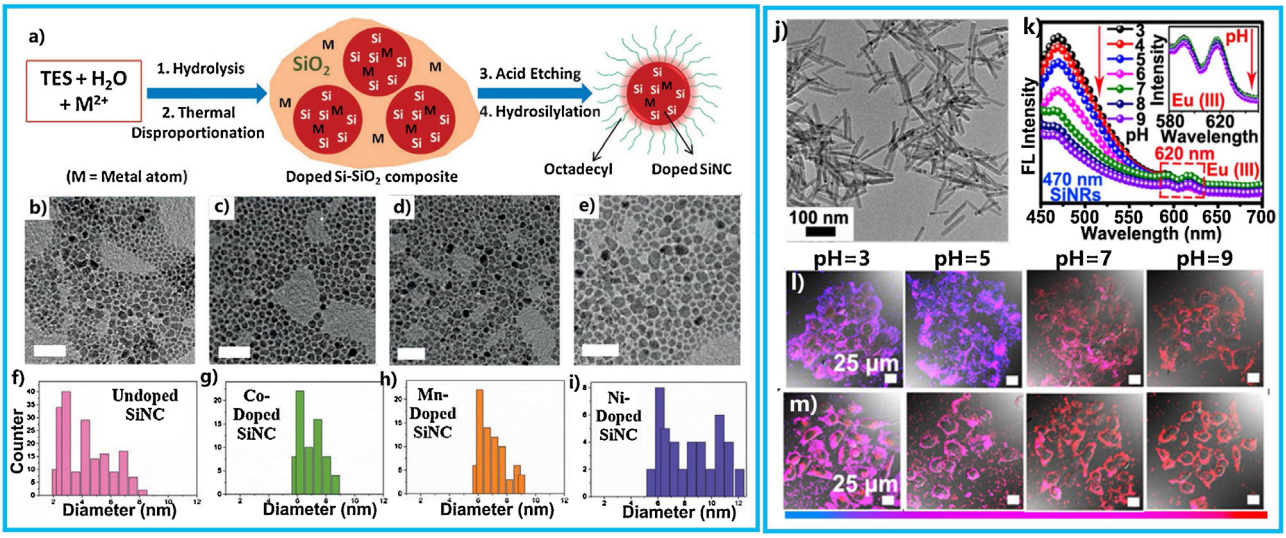

Fig. 6. (a) Illustration of the synthesis of octadecyl-modified metal doped SiNPs. TEM images of undoped (b), Co-doped (c), Mn-doped (d) and Ni-doped (e) SiNPs (reaction temperature: 1100 °C) (scale bars = 50 nm). (f–i) Size distribution analysis of the doped (c–e) and undoped (b) SiNPs. (*j*) TEM image of Eu-doped SiNRs. (k) PL spectra of Eu@SiNRs in PBS buffer with different pH values (3–9) using 405 nm excitation wavelength. Fluorescent bioimages of Eu-doped SiNRs in HeLa cells (l) and MCF-7 (m) cells at different pH values. (a–i) Printed with permission from Wiley Publications [103]; (j–m) Printed with permission from ACS Publications [104].

According to previous studies, metal-doped SiNPs could be prepared through a multi-step procedure, using Fe- or Mn-doped silicon precursor. In general, the resultant SiNPs doped with approximately ~0.5% metal exhibited blue emission. In 2017, Winnik and co-workers reported a novel kind of transition metal-doped SiNPs with no more than 0.2% metal atoms. This reported synthesis started with thehydrolysis/polymerization of triethoxysilane in the presence of an acidic transition metal salt aqueous solution (Ni^{2+}, Mn^{2+}, Co^{2+} and Cu^{2+}). The resulting $(HSiO_{1.5})_n$ gel loaded with transition metal ions was reacted through thermal disproportionation, hydrofluoric acid-etching and hydrosilylation with octadecene, producing undoped SiNPs (Fig. 6a). According to TEM characterizations, the transition metal-doped SiNPs were larger than the SiNPs with narrower size distribution. The size of SiNPs grown at 1100 °C ranged from 8.75:3.25 nm (Ni) and 7.5:1.5 nm (Mn) to 7.3:1.3 nm (Co), compared to 5.0:2.5 nm in the system of SiNPs (Fig. 6b-i). Their PL emission exhibited narrow bands, centered at 1000, 992 and 985 nm for Co, Ni, and Mn, respectively, which correspond to red-shifts of 82, 74 and 67 nm, compared to the PL wavelength of SiNPs (918 nm). Significantly, the resultant SiNPs emitted with absolute PLQY as high as ~26% within the red-to-near-infrared emission window. They attributed this result to the generation of nonradiative channels in doped SiNPs induced by the energy levels of the inserted Ni and Mn atoms. This result indicated that the energy levels of Co might hardly affect the emissive pathways of SiNP [103].

Very recently, Chu et al. developed a new kind of one-dimensional lanthanide doped SiNRs (Fig. 6j) through one-pot microwave irradiation-assisted synthesis. In this case, the surface groups (such as carboxyl) of SiNRs could provide plenty of chelation sites ready for reacting with Eu^{3+} ions. Therefore, the doped Eu could be sensitized by the carboxyl and other groups of SiNRs effectively, showing bright fluorescence, simultaneously realizing the integration of red and blue PL properties into a single structure (in general, europium ions could generate intense visible PL emission tuned by functional surface groups under UV irradiation, which was arising from f-d or f-f energy transfer.). In particular, the resultant Eu-doped SiNRs displayed pH-sensitive PL emission peak at 470 nm and pH-insensitive emission peak at 620 nm under the same excitation wavelength, thus producing self-correcting fluorescent signals (Fig. 6k).

Recently, great attention in the synthesis of fluorescent silicon nanomaterials has oriented to the explorations of integration of magnetic and fluorescent functions into a single nanosystem for multi-mode applications [91–99,105]. However, the synthesis of multi-functional one-dimensional silicon nanostructures simultaneously displaying unique fluorescent and magnetic properties is still in a high demand and seldom achieved, which might be attributed to the following two factors: (i) the doped magnetic species might induce negative effects to the fluorescent properties of silicon nanomaterials (e.g., the PLQY would significantly down to 1%) since the introduced magnetic species might act as magnetism-related optical trap localized in the band gap of fluorescent silicon nanomaterials; (ii) the strategy of synthesizing such hybrid one-dimensional silicon nanosystem generally contained rigorous experimental conditions and relatively tedious prepared procedures. To address these issues, He's group presented a novel kind of one-dimensional silicon nanoshuttles (SiNSs), simultaneously displaying attractive biocompatible, optical and magnetic properties. The SiNSs could be rapidly (~30 min) and readily prepared through in situ bottom-up growth through microwave reaction, by using APTMS and ferric trichloride ($FeCl_3$) as precursors. In particular, the as-prepared SiNSs featured strong fluorescence with PLQY of ~15%, with robust stabitliy and excitation-wavelength-dependent emission behavior. Besides of the attractive fluorescent properties, the resultant SiNSs featured paramagnetic properties at room temperature, showing prominent transverse (T_2) and longitudinal (T_1) relaxation contrast, with the ratio of longitudinal relaxivity (r_1) to transverse relaxivity (r_2) down to 1.56 (Fig. 7a–c) [105]. Such excellent fluorescent and magnetic properties made this as-prepared SiNSs a new kind of high-quality multi-functional ink for advanced anti-counterfeiting applications.

In the following studies, they further exploited the SiNSs-based anti-counterfeiting inks for printing fluorescent patterns. Encrypted numbers could be fabricated from the SiNP ink, SiNS ink and commercially available yellow fluorescent organic dye (Rhodamine 6 G) through inkjet printing method. Moreover, different fluorescent LCD characters could be observed under different excitation wavelength (Fig. 7(d–h)). In addition, MRI pore plates injected with contrast agents were imaged through 3.0 T magnetic resonance imaging. As shown in Fig. 7i–k, the characters "6 0 4″ were detected as bright signals in the T_1 image (Fig. 7j). The char-

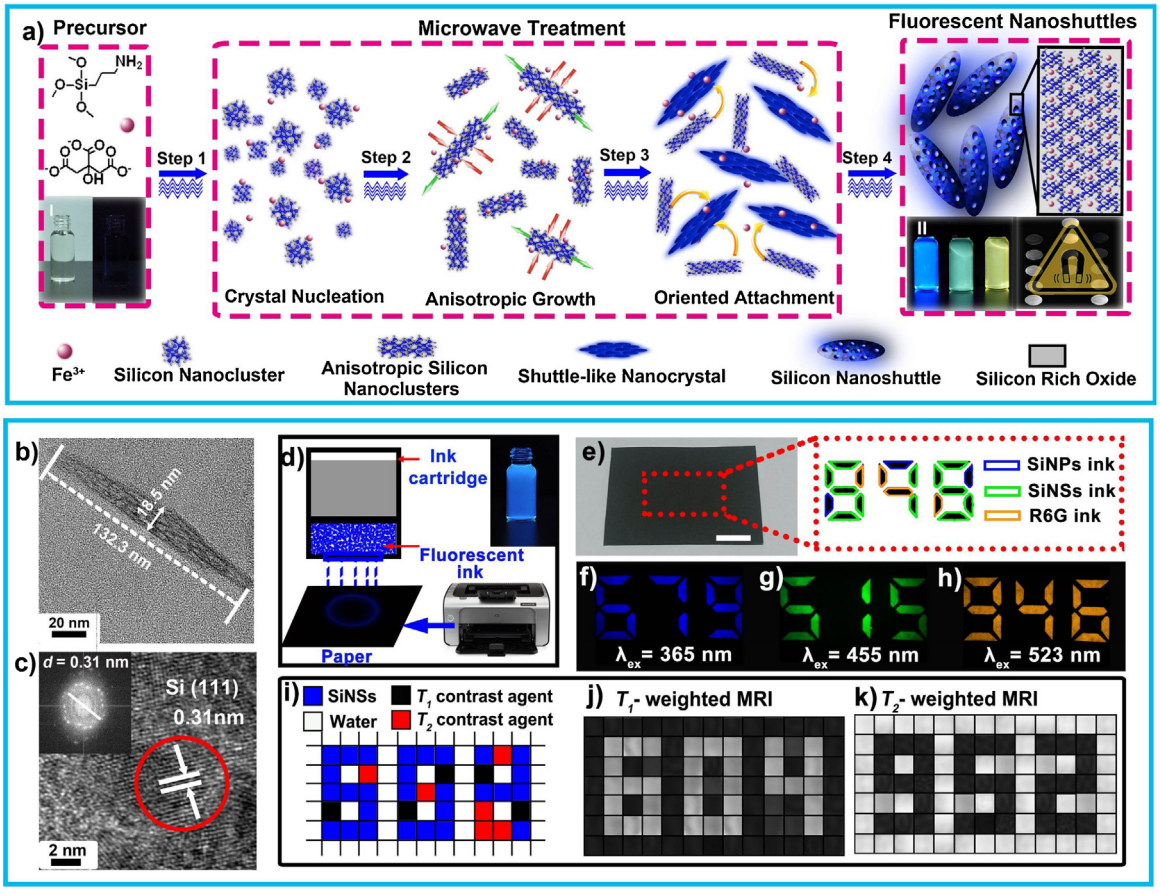

Fig. 7. (a) Illustration of the one-dimensional SiNSs through microwave synthesis (I: the images of the reaction precursor under the ambient light (left) and irradiation of UV (right). II: the fluorescent images of the SiNSs under different excitation wavelengths). TEM (b) and HRTEM (c) images of the SiNSs. (d) Illustration of inkjet printing procedures. Optical (e) and fluorescent photographs (f–h) on commercially available paper of numbers labeled by SiNSs, SiNPs and R6 G inks imaged with different excitation wavelengths. (i) Fabrication of well plates with different contrast agents. (*j*, k) T_1 and T_2 images of the anti-counterfeiting numbers. (a–c) Printed with permission from RSC Publications [105]. (d–k) Printed with permission from RSC Publications [106].

acters "9 5 2" were clearly observed through the T_2 images (Fig. 7k). These results suggested the SiNSs as a new kind of multi-functional ink for advanced anti-counterfeiting applications [106].

Biological species-modified fluorescent silicon nanomaterials

Fluorescent biological imaging is well-known as a powerful strategy for biological studies from cells to animals [16–19]. As mentioned in previous reports, biological species-modified silicon nanomaterials with bright fluorescence, robust stability and special biological functions have been fabricated as a new kind of high-performance fluorescent probes extensively for bioimaging in real-time and long-term manners [15,17–19]. Recent years have witnessed further achievements in the development of silicon nanomaterials featuring unique optical merits and specific biological functionalities [12–18].

During the past decade, scientists have made extensive efforts on evaluating biosafety assessment of fluorescent silicon nanomaterials. The favorable biocompatibility of silicon nanomaterials has been demonstrated in various animal models (e.g., elegans, mice and monkeys) [11–19,107]. In particular, previous reports have shown that small-sized (< ~10 nm) SiNPs could be biodegraded to orthosilicic acid (renal clearable components, which are naturally found in human tissues) and readily excreted from the body through the urine [108,109]. Of note, in January 2011, SiNPs with small size (~3-10 nm) received the approved investigational new drug approval for the first-in-human clinical trial from the Food and Drug Administration (FDA) (NCT01266096, NCT02106598) [110]. These exciting achievements suggest the biological species-modified fluorescent SiNPs as biocompatible fluorescent nanoprobes, holding great promise for biomedical and biosensor applications.

Recently, gene therapy is reported to be a high-efficacy method for the treatment of severe diseases [111,112]. To date, various fluorescent nanomaterials have been extensively exploited as gene carriers [113–116]. However, several issues (e.g., potential cytotoxicity and photobleaching properties) need to be further addressed for allowing the long-term tracking and analysis of the intracellular behavior of gene vectors. In 2018, Ji et al. developed a kind of fluorescent and biocompatible protamine sulfate (PS)-coated SiNP (PS@SiNP)-based gene nanocarrier (Fig. 8a). Significantly, the resultant PS@SiNP-based gene carriers featured strong fluorescence (PLQY: ~25%) with robust stability. Taking advantages of the excellent optical properties of PS@SiNP, the nuclear import of PS@SiNP-pDNA gene carriers and gene expression could be successfully tracked at subcellular manner (Fig. 8b). Significantly, the dissociation of pDNA from the PS@SiNP-pDNA gene carriers in living cells could be vividly explored by tracking the optical signals from SiNPs. Based on the long-term (30 h) tracking of gene release and transport in living cells, the authors revealed the PS/plasmid DNA ratio-and time-dependent intracellular behavior of PS@SiNPs [117].

One of the important goals in biomedicine is the ability to perform multi-functions through the all-in-one nanoprobe, that is, the ability to monitor disease progress, image and target using only single entity [17–19]. In 2018, Santos and co-workers reported a

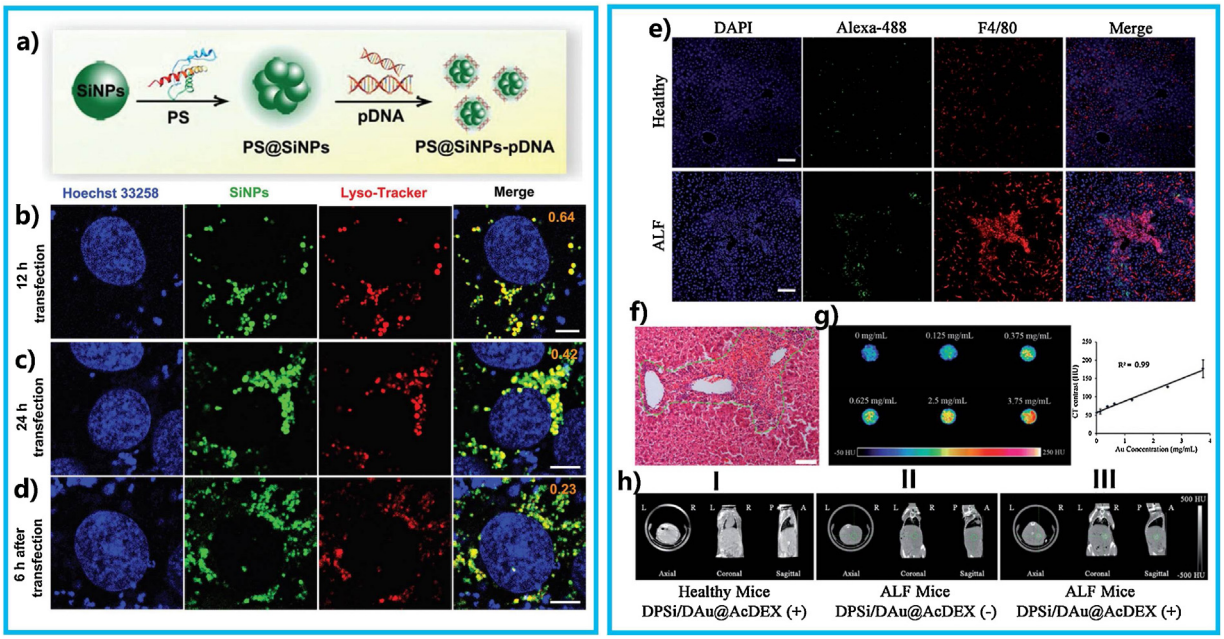

Fig. 8. (a) Illustration of the synthesis of PS@SiNPpDNA-based gene carriers. Fluorescent bioimages of the subcellular location of PS@SiNP-pDNA-based gene carriers in ARPE-19 cells after staining for various times (12 h (b) and 24 h (c) and 6 h after the 24 h transfection period (d)). The fluorescent signal of SiNPs, LysoTracker Red DND-99 and Hoechst 33,258 was defined as green color, red color and blue color, respectively. The merged fluorescent bioimages displayed the colocalization between the green fluorescence from SiNPs and red fluorescence from LysoTracker. Scale bars = 5 μm. (e) Immunofluorescence bioimages of ALF liver and healthy liver after treatment with Alexa-488-labeled DPSi/DAu@AcDEX. Scale bar = 100 μm. (f) H&E labeling of ALF liver, demonstrating the lesion-specific-macrophages accumulation. Scale bar = 100 μm. (g) The CT images and values of the DPSi/DAu@AcDEX with different concentrations. (h) In vivo CT images of ALF mice after treatment of DPSi/DAu@AcDEX (-), ALF mice after treatment of DPSi/DAu@AcDEX (+) and healthy mice after treatment of DPSi/DAu@AcDEX (+). (a–d) Printed with permission from RSC Publications [117]. (e–h) Printed with permission from Wiley Publications [118].

novel kind of hybrid nanosystem based on SiNPs, gold nanoparticles (AuNPs), and acetalated dextran (DPSi/DAu@AcDEX) to enhance the computer tomography (CT) signal, deliver and encapsulate one drug for acute-liver-failure (ALF) diagnosis and treatment. This nanosystem could be used to determine pathologically change behaviors in the tissues and deliver therapeutic species to the target sites selectively. The functional hybrid nanosystem further optimized the drug solubility, delivery and treatment time. In addition, the residence of AuNPs within the therapeutic species further facilitated this nanosystem for further CT-imaging. Therefore, these results supported that this silicon-based hybrid nanosystem was highly promising for diagnosis and treatment of ALF (Fig. 8e–h) [118].

In clinic trial, neovascular eye diseases were usually diagnosed by fluorescein angiograph and then treated through multi-intravitreal injections [119–123]. In addition, the lack of long-term and real-time tracking disease progress and corresponding assessment of therapeutic studies further impede the healing of neovascular eye diseases. In 2018, Tang and co-workers presented a kind of theranostic agents made of (c-(RGDyC))-conjugated SiNPs (SiNPs-RGD), which featured unique antiangiogenic ability in transwell invasion, wound healing migration, tube formation assays and transwell migration. Then such SiNPs-RGD were further developed as high-performance agents for neovascularization inhibition and labeling the blood vessels through a synchronous manner. In mouse corneal angiogenesis model, the SiNPs-RGD featured attractive binding ability to angiogenic blood vessels (Fig. 9a-c). In antiangiogenic activity study, the SiNPs-RGD-treated mode displayed distinct suppression after 7 d post-injection, which showing stable and significant inhibition of blood-vessel condition (Fig. 9d and e). The quantitative analysis of suppression of vessel lengths showed that the blood-vessel lengths were suppressed in SiNPs-RGD-treated group and further reached 3.23 ± 0.60 mm on day 14, indicating the high efficacy of corneal neovascularization treatment (Fig. 9f). These conclusions indicated that SiNPs-RGD-based nanosystem was a potential diagnosis and treatment nanoplatform for neovascular eye diseases [123]. Moreover, silica NPs, known as another kind of high-quality silicon-based materials whose luminescent mechanism is different from silicon NPs (Both silica and silicon SiNPs have excellent biocompatibility due to negligible toxicity of silicon), were also demonstrated to feature anti-angiogenic properties [124–126]. Typically, Leong and co-workers showed that the endothelial cells angiogenic behavior could be elegantly restricted through silica nanoparticle. This anti-angiogenesis property was originated from the diameter dependent uptake of silica nanoparticles and generation of reactive oxygen species that influenced by p53 tumor suppressor channel [125]. Similarly, Kim and collaborators demonstrated that silica nanoparticles suppress pathological angiogenesis mainly induced by VEGF in the retina [126].

It is worth noting that although the SiNPs featured excellent fluorescent properties, additional functional species are still necessary for providing the SiNPs with special functions [127,128]. In the past few years, the combination of fluorescent silicon nanomaterials and traditional cancer therapeutics has solved many challenges in biology and biomedicine fields [129,130]. In particularly, for thousands of years, the rich natural species of traditional Chinese medicines (TCMs) have produced many kinds of anticancer agents, featuring a significant position in treating and preventing cancer and related diseases. Compare to the traditional cancer therapeutics that are regarded as potentially unsafe to the environment and human body, TCM compounds are more attractive, not only because they are better cultural acceptability, but also due to their rich resources and excellent compatibility with the human life system [131–136]. In the latest study, Ji et al. introduced a novel method, i.e., TCM (5-hydroxy-2-methyl-1,4-naphthoquinone ($C_{11}H_8O_3$, plumbagin (PLB), from Plumbago indica) (Fig. 9g)-assisted microwave reaction, for the one-pot synthesis of fluorescent anti-cancer SiNPs

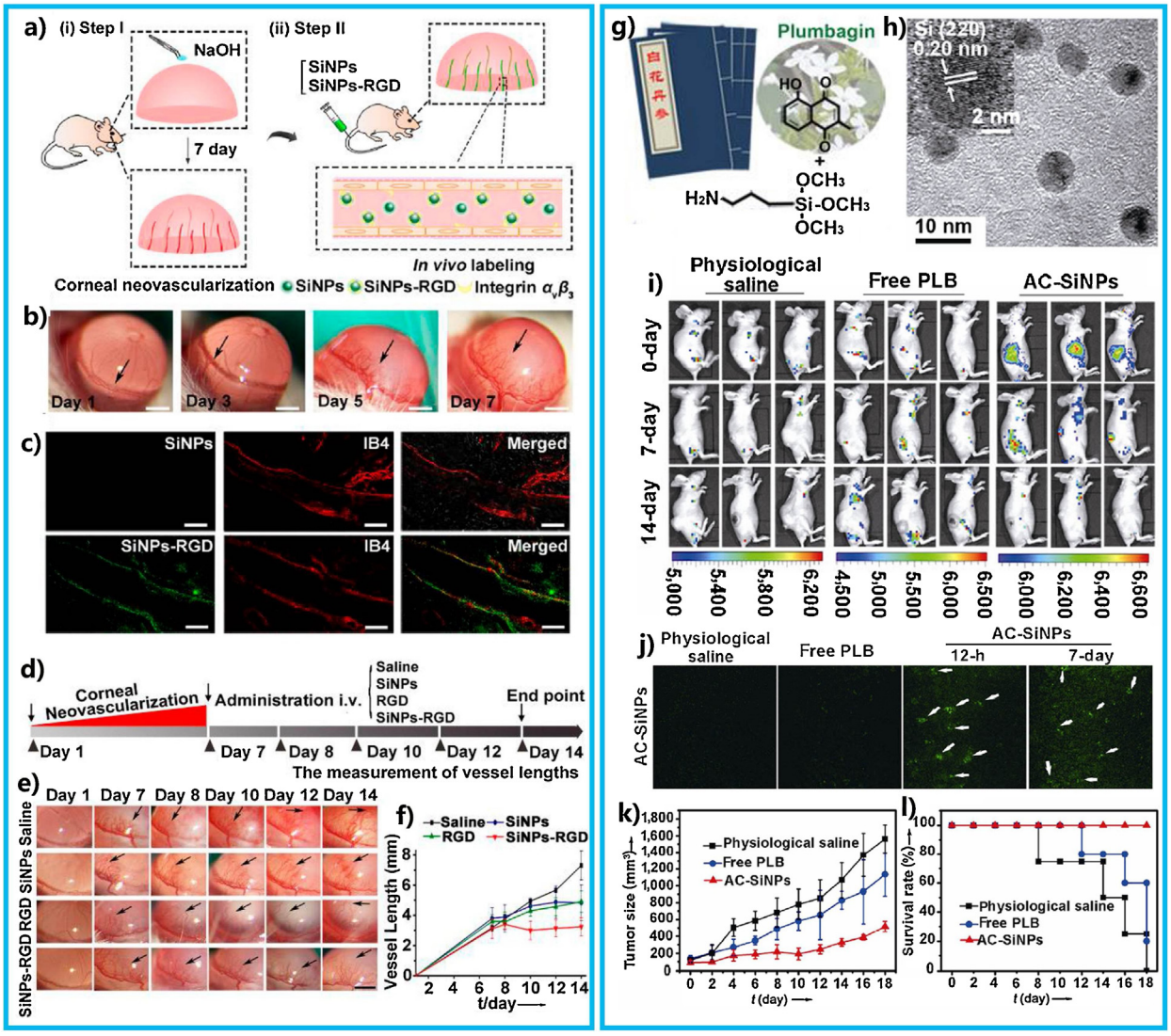

Fig. 9. (a) Illustration of the anti-angiogenic blood vessels ability of SiNPs and SiNPs-RGD. (b) Photographs of corneal neovascularization through injury treatment. Scale bar = 5 mm. (c) Fluorescent bioimages of angiogenic blood vessels after intravenous treatment with SiNPs-RGD (lower) and pure SiNPs (upper). Scale bar = 25 μm. (d) The process of inhibition of corneal neovascularization. (e) Photographs of mice corneas after alkali-inducd injury and intravenous treated with pure SiNPs-RGD, SiNPs, physiological saline and c(RGDyC). Scale bar = 2 mm. (f) Quantitative results of vessel sizes of different treatment groups. (g) Schematic diagram of the AC-SiNPs precusor. (h) HRTEM and TEM characterizations of the resultant AC-SiNPs. (i) In vivo bioimages of mice after AC-SiNPs, PLB and physiological saline treatment during different time. (j) Histological analysis of AC-SiNP treatment in 4T1 tumor. 4T1 tumor growth rate (k) and survival spectra (l) of the mice treated with AC-SiNPs, free PLB, and saline.(a–f) Printed with permission from ACS Publications [123]. (g–k) Printed with permission from Springer Publications [137].

(AC-SiNPs). Particularly, the resultant AC-SiNPs exhibited small-size (diameter: ~3.7 nm) (Fig. 9h), good water solubility, high fluorescence (PLQY: ~15%), as well as robust storage- and photo-stability. Particularly, the quinone groups in AC-SiNPs would induce increased accumulation of ROS towards cancer cells, inducing distinct cancer cells death. Taking advantages of the excellent optical properties and intrinsic anti-tumor function with good selectivity, the resultant AC-SiNPs were further explored to be especially applicable for real-time and long-term tracking and treatment of cancer with high efficiency. In animal experiment, the distinct and stable fluorescent signals from AC-SiNPs in the cancer sites could be observed after 7 days post-injection (Fig. 9i and *j*), which was advantageous to the suppression of tumor growth and long-lasting resistance of cancer cells. Moreover, the tumor sizes analysis and the calculated survival results of mouse during the 18-day detection further demonstrated the intrinsic anti-cancer efficacy of the AC-SiNPs (Fig. 9k and l) [137].

Taking advantages ofred blood cells (RBCs) with long circulation, Jiang and co-workers developed a kind of smart drug delivery based on DOX-loaded SiNPs encapsulated into RBCs (SiNPs-DOX@RBCs). The resultant system simultaneously exhibited excellent fluorescent properties and lengthened blood residency. Particularly, the SiNPs-DOX@RBCs had an obvious longer blood circulation time (7.31 ± 0.96 h) (3.9-fold longer than that of SiNPs-DOX), which could improve the accumulation of DOX in tumors [138]. The authors deduced that such drug nanocarriers could reach the correct tumor tissue site through the "nanoparticles-induced endothelial leakiness (NanoEL)" effect, which has been elaborately illustrated in recent reports [139–144].

In general, public health has been overwhelmed by many kinds of bacterial infections. Moreover, a new global threat during the combat with bacteria has appeared with the increasing incidence of drug resistance and antibiotic combined with the lack of efficient antibacterial agent in the clinic trial [145–149]. A consensus has

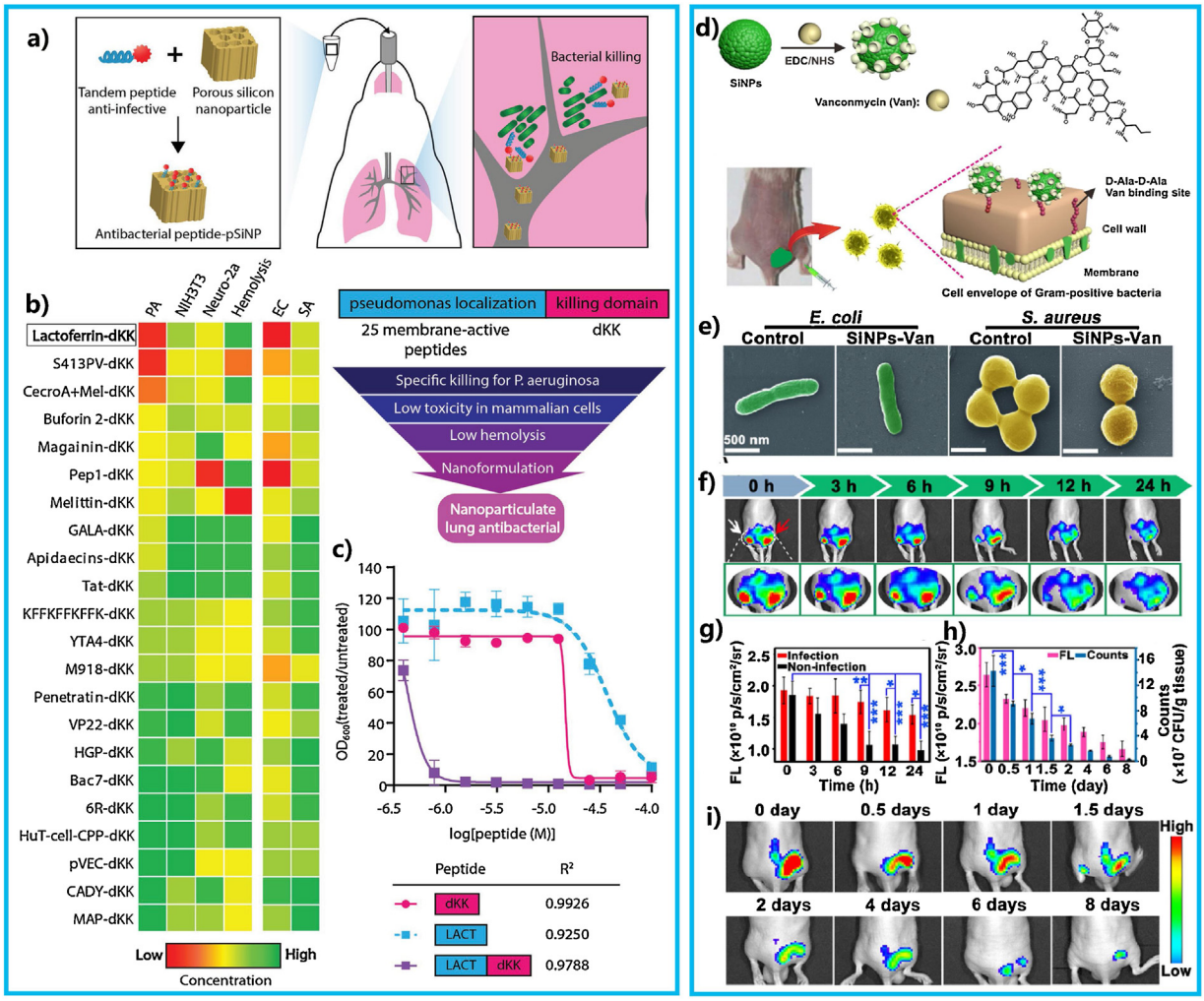

Fig. 10. (a–c) Illustration of the selection of tandem peptide. (a) The strategy was to prepare materials hybrid of anti-infective peptide loaded in fluorescent SiNPs for transportation to infective lung targets. (b) Tandem peptides have the capacity to restrain bacteria efficiently and low toxicity to the tissue would be selected as candidates for against P. aeruginosa. (c) MIC assay comparation of individual peptide domains (LACT and dKK) and LACT-dKK tandem peptide (the anti-bacterial turbidity was characterized during 14 h). (d) Illustration of the fabrication of SiNPs-Van and their capacity to realize Gram-positive bacteria-targeted bioimaging. (e) SEM characterization of S. aureus and E. coli and stained with SiNPs-Van and SiNPs. (f) In vivo fluorescent bioimaging of uninfected sites (left) and infected sites (right) stained with SiNPs-Van after different time and (g) time-dependent fluorescent intensity curves of uninfected or infected targets. (h) Long-term in vivo fluorescent bioimaging of S. aureus-infected mouse model after SiNPs-Van treatment and (i) time-dependent fluorescent intensity at infected points. (a–c) Printed with permission from Wiley Publications [150]. (d–i) Printed with permission from Springer Publications [151].

been reached that if bacterial infections could be effectively diagnosed and controlled at early stage, the lethality from infections could be dramatically decreased. Recently, Bhatia and co-workers demonstrated a tandem peptide-based antibacterial agent with unique synergistic activity; the efficacy of the anti-infective was more than 30-fold higher than their individual components. They utilized the best performing agent into a biocompatible fluorescent SiNPs, and obtained great decreases in bacteria titers when delivery to the lung in a mouse model of lung bacterial infection. The clinical isolated from human lung bacterial infection were susceptible to peptide killing, indicating that this SiNPs-based anti-infective might be efficacious to different kinds of strains of P. aeruginosa (Fig. 10a-c) [150].

In 2018, Zhai and co-workers presented a new fluorescent SiNPs-based theranostic nanoprobe whose surface was functionalized with vancomycin (SiNPs-Van) (Fig. 10d and e). The as-prepared nanoprobes were capable of noninvasive and prolonged fluorescence imaging, activity targeted and high-efficacy treatment of bacteria. In this study, SiNPs were able to stain Gram-positive bacteria selectively with robust photostability. Taking advantage of the excellent properties from SiNPs, they further employed the unique resultant SiNPs-Van probes for long-term in vivo tracking of S. aureus infections (Fig. 10f-h). By virtue of good specificity and photostability of SiNPs, the nanoprobes had the ability to track S. aureus infections in vivo for a long-lasting period (8 days), indicating the lengthy retention of SiNPs in infected sites (Fig. 10i) [151].

Conclusion and outlook

In this review, we aim to summary the latest relevant progress toward the synthesis, functionalization and optical applications of fluorescent silicon nanomaterials. Firstly, the last decade has witnessed the significant development in the synthesis of fluorescent silicon nanomaterials. As mentioned in Section 1, (1) Microwave reaction provided an efficacious way for rapid preparation of high-quality SiNPs, e.g., ~0.1 g SiNPs are readily prepared in a ~10 min reaction. (2) Photochemical synthesis realized a low-cost synthetic method under mild-condition capable of large-scale production (~10 g/40 min) of fluorescent SiNPs. (3) Biomimetic preparation suggested new opportunities for the synthesis of flu-

orescent SiNPs from biocompatible biomass precursors (the global supply of diatoms has been estimated about ~10 000 000 t every year). (4) One-step in situ growth of fluorescent SiNPs in common glass bottle under atmospheric pressure and room temperature provided a more facile synthetic approach without harsh reaction condition and additional instruments. As discussed in Section 2, a number of methods have been developed for preparing one-dimensional fluorescent SiNRs, among which ligand-assisted SLS growth method and microwave synthesis are recognized as well-developed approaches capable of the preparation of high-quality SiNRs with high production yield. While fluorescent silicon nanomaterials have shown great promise for various applications, there still remain a number of vital challenges facing reasonable design of well-defined fluorescent silicon nanostructures, sophisticated preparation of multifunctional properties and systematic biosafety assessment for the promotion in clinical field. Despite the progresses of preparation of fluorescent silicon nanomaterials, extensive explorations are still necessary to address following significant issues, including: (1) The convincing optical mechanism of silicon nanomaterials is still need to be addressed. (2) Researchers should put continuous efforts on controllable synthesis of SiNRs with desirable sizes and lengths. (3) The thorough understanding of growth kinetics of fluorescent zero- or one-dimensional silicon nanomaterials is necessary.

In addition, multifunctional silicon nanomaterials have been designed with desirable features (e.g., ultrahigh PLQYs and electronic/magnetic properties). These kinds of well-established multifunctional silicon nanostructures impart important contribution to the development of silicon nanotechnology, opening up exciting avenues in a verity of applications. Moreover, based on previously reports and our recent efforts, we hold the opinion that the surface ligands would serve as an important factor to the optical properties of SiNPs (such as PLQY). It has been shown that through reasonable functionalization, the surface modification of SiNPs with nitrogen element-capped ligands leads to the high PLQY of up to 70–90%. The PL in these species is shown to arise from CT states between the silicon surface and ligands. This phenomenon could be used in a theoretical fashion for rational design and preparation of SiNPs with a wider range of PL wavelengths. Moreover, it is attractive to blend multi-functions into single silicon nanosystem. Many studies have realized successful doping of metal ions into silicon nanosystems to achieve multifunctional silicon nanomaterials. However, sufficient experimental and theoretical data are still necessary to clearly testify the relationship between functional species and properties of fluorescent silicon nanomaterials, which would be vastly helpful for the fabrication and design of fluorescent silicon nanomaterials with required functionalities. Furthermore, several kinds of biological species-modified silicon nanomaterials have been developed as a new kind of fluorescent probes for monitoring dynamic biological behaviors in real-time and long-term manners. Moreover, the biological functional silicon nanomaterials have emerged as high-efficacy therapeutic agent for treatment of diseases with exciting outcomes.

In the outlook section, we provide the perspective of functional silicon nanomaterials in optical applications (Scheme 2). It is worth pointing that the resolution of bioimaging can be significantly enhanced by using time-gating techniques due to the minimizing interference from autofluorescence. Therefore, preparing silicon nanomaterials with long-lived phosphorescence would be attractive for high-resolution bioimaging. Moreover, *in vivo* NIR fluorescence imaging is emerging as an attractive imaging modality with high resolution, owing to its advances in reducing photon scattering, light absorption and autofluorescence [152–154]. Recently, the two-photon imaging has also been developed in silicon nanosystem [155]. Therefore, the exploration of SiNPs-based near infrared (NIR) and/or two-photon imaging

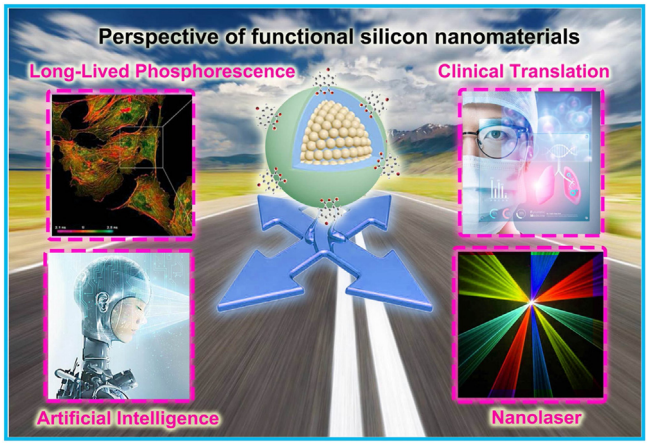

Scheme 2. Perspective of silicon nanomaterials in optical applications.

techniques would further facilitate the improvement of imaging solution and sensitivity. Plenty of studies have focused on preparing silicon nanomaterials with biological species functionalized as high-quality fluorescent tracking and nanoagent system for diagnosis and therapy of diseases. It is also worth mentioning that, to take advantages of excellent fluorescent properties (e.g., high and stable fluorescence) and negligible toxicity, such high-quality fluorescent silicon nanomaterials would serve as novel promising tools in the field of neuroscience, which has been intensively studied in recent years [156–160]. Typically, based on the strong and stable optical signals of silicon nanomaterials, the dynamic behavior of neurons might be clarified in long-term manner. Secondly, the rich surface functionalization of silicon nanomaterials may further facilitate the subcellular molecular fluorescent markers of neurons, providing valuable information of neuronal disease. Moreover, we believe that silicon nanomaterials with special optical and neuronal functions would provide a new possibility for high-sensitivity fluorescence sensing towards brain activity.

On the other hand, unique optical information of silicon nanomaterias could be collected and used as valid input data for fluorescent signal-based artificial intelligence response application, which potentially helping artificial intelligence to output decisions in efficient manners. Finally, one-dimensional silicon nanostructure with lower thresholds for multiexction generation and optical gain exhibit potentially opportunity for fabricating high-efficiently devices and nanolaser.

In summary, fluorescent silicon nanomaterials have shown their unique advantages and excellent performance in various optical applications. Despite of the exciting research progresses on the development of silicon nanomaterials, some issues which might impede the practical use of silicon nanomaterials are still required to be addressed, including: 1. Accurate optical mechanism of silicon nanomaterials needs to be clearly and convincingly clarified, providing valuable guidance for the synthesis of fluorescent silicon nanomaterials with tunable fluorescent properties. 2. Large-scale and controllable synthesis of silicon nanomaterials with high PLQY (particular in NIR (800–1400 nm) window)is still in high demand for high-resolution bioimaging application. 3. Researchers should make continuous exploration on designing functional species for rational surface modifications, facilitating the preparation of silicon nanomaterials with special functionalities and well-defined structures. 4. Comprehensive and reliable biosafety assessment is essentially required for wide-ranging practical applications.

We anticipate that the fast development of new silicon-based nanotechniques will lead to significant improvements of silicon nanotechnology, opening new avenues for long-awaited silicon-based optical applications.

Acknowledgments

We appreciate financial support from the National Natural Science Foundation of China (21825402, 31400860, 21575096, and 21605109), The Natural Science Foundation of Jiangsu Province of China (BK20170061), and a project funded by the Priority Academic Program Development of Jiangsu Higher Education Institutions (PAPD), 111 Project as well as Collaborative Innovation Center of Suzhou Nano Science and Technology (NANO-CIC).

References

[1] L. Canham, Nature 408 (2000) 411–412.
[2] Q. Qing, Z. Jiang, L. Xu, R.X. Gao, L.Q. Mai, C.M. Lieber, Nat. Nanotechnol. 9 (2014) 142–147.
[3] C. Chiappini, D.E. Rosa, J.O. Martinez, X. Liu, J. Steele, M.M. Stevens, et al., Nat. Mater. 14 (2015) 532–539.
[4] F. Patolsky, B.P. Timko, G.H. Yu, Y. Fang, A.B. Greytak, G.F. Zheng, et al., Science 313 (2006) 1100–1104.
[5] A.G. Cullis, L.T. Canham, Nature 353 (1991) 335–338.
[6] P.D. Howes, R. Chandrawti, M.M. Stevens,Science 346 (2014), 1247390.
[7] G.F. Grom, D.J. Lockwood, J.P. McCaffrey, H.J. Labbe, P.M. Fauchet, B. White, et al., Nature 407 (2000) 358–361.
[8] Z. Ding, B.M. Quinn, S.K. Haram, L.E. Pell, B.A. Korgel, A.J. Bard, Science 296 (2002) 1293–1297.
[9] N.M. Park, C.J. Choi, T.Y. Seong, S.J. Park, Phys. Rev. Lett. 86 (2001) 1355–1357.
[10] W.L. Wilson, P.F. Szajowski, L.E. Brus, Science 262 (1993) 1242–1244.
[11] M. Montalti, A. Cantelli, G. Battistelli, Chem. Soc. Rev. 44 (2015) 4853–4921.
[12] X.Y. Cheng, S.B. Lowe, P.J. Reece, J.J. Gooding, Chem. Soc. Rev. 43 (2014) 2680–2700.
[13] B.F.P. McVey, R.D. Tilley, Acc. Chem. Res. 47 (2014) 3045–3051.
[14] M. Dasog, J. Kehrle, B. Rieger, J.G.C. Veinot, Angew. Chem. Int. Ed. 55 (2016) 2322–2339.
[15] F. Peng, Y.Y. Su, Y.L. Zhong, C.H. Fan, S.T. Lee, Y. He, Acc. Chem. Res. 47 (2014) 612–623.
[16] J.D. Holmes, K.J. Ziegler, R.C. Doty, L.E. Pell, K.P. Johnston, B.A. Korgel, J. Am. Chem. Soc. 123 (2001) 3743–3748.
[17] Y.Y. Su, X.Y. Ji, Y. He, Adv. Mater. 28 (2016) 10567–10574.
[18] X.Y. Ji, H.Y. Wang, B. Song, B.B. Chu, Y. He, Front. Chem. 6 (2018) 38–46.
[19] Y. He, Y.Y. Su, Silicon Nano-biotechnology, Springer, Berlin, 2014.
[20] Z.H. Kang, C.H.A. Tsang, Zhang Z, M. Zhang, N. Wong, J.A. Zapien, et al., J. Am. Chem. Soc. 129 (2007) 5326–5327.
[21] C.S. Yang, R.A. Bley, S.M. Kauzlarich, H.W. Lee, G.R. Delgado, J. Am. Chem. Soc. 121 (1999) 5191–5195.
[22] M. Dasog, G.B. De los Reyes, L.V. Titova, F.A. Hegmann, J.G.C. Veinot, ACS Nano 8 (2014) 9636–9648.
[23] D. Riabinina, C. Durand, M. Chaker, F. Rosei,Appl. Phys. Lett. 88 (2006), 073105.
[24] A. Shiohara, S. Hanada, S. Prabakar, K. Fujioka, T.H. Lim, K. Yamamoto, et al., J. Am. Chem. Soc. 132 (2010) 248–253.
[25] L. Mangolini, E. Thimsen, U. Kortshagen, Nano Lett. 5 (2005) 655–659.
[26] N. Arul Dhas, C.P. Raj, A. Gedanken, Chem. Mater. 10 (1998) 3278–3281.
[27] T.M. Atkins, A. Thibert, D.S. Larsen, S. Dey, N.D. Browning, S.M. Kauzlarich, J. Am. Chem. Soc. 133 (2011) 20664–20667.
[28] Y. He, Z.H. Kang, Q.S. Li, C.H.A. Tsang, C.H. Fan, S.T. Lee, Y. He, Angew. Chem. Int. Ed. 48 (2009) 128–132.
[29] Y. He, Y. Zhong, F. Peng, X. Wei, Y. Su, Y. Lu, et al., J. Am. Chem. Soc. 133 (2011) 14192–14195.
[30] Y. Zhong, F. Peng, F. Bao, S. Wang, X. Ji, L. Yang, Y. Su, S.T. Lee, Y. He, J. Am. Chem. Soc. 135 (2013) 8350–8356.
[31] J.L. Heinrich, C.L. Curtis, G.M. Credo, M.J. Sailor, K.L. Kavanagh, Science 255 (1992) 66–68.
[32] D. Nesheva, C. Raptis, A. Perakis, I. Bineva, Z. Aneva, Z. Levi, S. Alexandrova, H. Hofmeister, J. Appl. Phys. 92 (2002) 4678–4683.
[33] B. Garrido, C. Garcia, S.Y. Seo, P. Pellegrino, D. Navarro-Urrios, N. Daldosso, L. Pavesi, F. Gourbilleau, R. Rizk, Phys. Rev. B Condens. Matter Mater. Phys. 76 (2007), 245308.
[34] S.M. Liu, Y. Yang, S. Sato, K. Kimura, Chem. Mater. 18 (2006) 637–642.
[35] S.M. Liu, S. Sato, K. Kimura, Langmuir 21 (2005) 6324–6329.
[36] C.M. Hessel, E.J. Henderson, J.G.C. Veinot, Chem. Mater. 18 (2006) 6139–6146.
[37] C.M. Hessel, M.A. Summers, A. Meldrum, M. Malac, J.G.C. Veinot, Adv. Mater. 19 (2007) 3513–3516.
[38] C.M. Hessel, D. Reid, M.G. Panthani, M.R. Rasch, B.W. Goodfellow, J. Wei, Chem. Mater. 24 (2012) 393–401.
[39] J.R. Heath, Science 258 (1992) 1131–1133.
[40] J.P. Wilcoxon, G.A. Samara, P.N. Provencio, Phys. Rev. B Condens. Matter Mater. Phys. 60 (1990) 2704–2714.
[41] D. Mayeri, B.L. Phillips, M.P. Augustine, S.M. Kauzlarich, Chem. Mater. 13 (2001) 765–770.
[42] R.K. Baldwin, K.A. Pettigrew, J.C. Garno, P.P. Power, G.Y. Liu, S.M. Kauzlarich, J. Am. Chem. Soc. 124 (2002) 1150–1151.
[43] R.A. Bley, S.M. Kauzlarich, J. Am. Chem. Soc. 118 (1996) 12461–12462.
[44] J. Zou, R.K. Baldwin, K.A. Pettigrew, S.M. Kauzlarich, Nano Lett. 4 (2004) 1181–1186.
[45] Y.L. Zhong, X.T. Sun, S.Y. Wang, F. Peng, F. Bao, Y.Y. Su, et al., ACS Nano 9 (2015) 5958–5967.
[46] S.C. Wu, Y.L. Zhong, Y.F. Zhou, B. Song, B.B. Chu, X.Y. Ji, et al., J. Am. Chem. Soc. 137 (2015) 14726–14732.
[47] Y.L. Zhong, B. Song, F. Peng, Y.Y. Wu, S.C. Wu, Y.Y. Su, et al., Chem. Commun. 52 (2016) 13444–13447.
[48] K.Q. Peng, X. Wang, L. Li, Y. Hu, S.T. Lee, Nano Today 8 (2013) 75–97.
[49] J. Resasco, N.P. Dasgupta, J.R. Rosell, J.H. Guo, P.D. Yang, J. Am. Chem. Soc. 136 (2014) 10521–10526.
[50] X.F. Duan, Y. Huang, R. Agarwal, C.M. Lieber, Nature 421 (2003) 241–245.
[51] A.I. Hochbaum, P.D. Yang, Chem. Rev. 110 (2010) 527–546.
[52] Y. Cui, Q. Wei, H. Park, C.M. Lieber, Science 293 (2001) 1289–1292.
[53] J.Y. Zheng, Y.L. Yan, X.P. Wang, Y.S. Zhao, J.X. Huang, J.N. Yao, J. Am. Chem. Soc. 134 (2012) 2880–2883.
[54] K.F. Wu, Y.L. Du, H. Tang, Z.Y. Chen, T.Q. Lian, J. Am. Chem. Soc. 137 (2015) 10224–10230.
[55] A. Shabaev, C.S. Hellberg, A.L. Efros, Acc. Chem. Res. 46 (2013) 1242–1251.
[56] L. Brus, P. Szajowski, W. Wilson, T. Harris, S. Schuppler, P.J. Citrin, J. Am. Chem. Soc. 117 (1995) 2915–2922.
[57] M. Govoni, I. Marri, S. Ossicini, Nat. Photonics 6 (2012) 672–679.
[58] M.T. Trinh, R. Limpens, W.D.A.M. de Boer, J.M. Schins, L.D.A. Siebbeles, T. Gregorkiewicz, Nat. Photonics 6 (2012) 316–321.
[59] A.T. Heitsch, D.D. Fanfair, H.Y. Tuan, B.A. Korgel, J. Am. Chem. Soc. 130 (2008) 5436–5437.
[60] A.T. Heitsch, C.M. Hessel, V.A. Akhavan, B.A. Korgel, Nano Lett. 9 (2009) 3042–3047.
[61] C.M. Hessel, A.T. Heitsch, B.A. Korgel, Nano Lett. 10 (2010) 176–180.
[62] A.M. Chockla, K.C. Klavetter, C.B. Mullins, B.A. Korgel, Chem. Mater. 24 (2012) 3738–3745.
[63] X. Lu, C.M. Hessel, Y. Yu, T.D. Bogart, B.A. Korgel, Nano Lett. 13 (2013) 3101–3105.
[64] X. Lu, B.A. Korgel, Chem. Eur. J. 20 (2014) 5874–5879.
[65] X.T. Lu, K.J. Anderson, P. Boudjouk, B.A. Korgel, Chem. Mater. 27 (2015) 6053–6058.
[66] B. Song, Y.L. Zhong, S.C. Wu, B.B. Chu, Y.Y. Su, Y. He, J. Am. Chem. Soc. 138 (2016) 4824–4831.
[67] C. Qian, W. Sun, L. Wang, C. Chen, K. Liao, W. Wang, et al., J. Am. Chem. Soc. 136 (2014) 15849–15852.
[68] J. Rinck, D. Schray, C. Kübel, A.K. Powell, G.A. Ozin, Small 11 (2015) 335–340.
[69] Q. Li, Y. He, J. Chang, L. Wang, H.Z. Chen, Y.W. Tan, et al., J. Am. Chem. Soc. 135 (2013) 14924–14927.
[70] L. Wang, Q. Li, H.Y. Wang, J.C. Huang, R. Zhang, Q.D. Chen, et al., Light Sci. Appl. 4 (2015) e245.
[71] Q. Li, T.Y. Luo, M. Zhou, H. Abroshan, J.C. Huang, H.J. Kim, et al., ACS Nano 10 (2016) 8385–8393.
[72] J.M. Lauerhaas, M.J. Sailor, Science 261 (1993) 1567–1568.
[73] J.M. Lauerhaas, G.M. Credo, J.L. Heinrich, M.J. Sailor, J. Am. Chem. Soc. 114 (1992) 1911–1912.
[74] W.Y. So, Q. Li, C.M. Legaspi, B. Redler, K.M. Koe, R.C. Jin, et al., ACS Nano 12 (2018) 7232–7238.
[75] H.J. Monkhorst, J.D. Pack, Phys. Rev. B 13 (1976) 5188–5192.
[76] X.B. Shen, B. Song, B. Fang, X. Yuan, Y.Y. Li, S.Y. Wang, et al., Nano Res. 11 (2018), doi: s12274-018-2217-3.
[77] Y.L. Zhong, B. Song, X.B. Shen, D.X. Guo, Yao He, Chem. Commun. 54 (2018), http://dx.doi.org/10.1039/C8CC07340F.
[78] X.B. Shen, B. Song, B. Fang, A.R. Jiang, S.J. Ji, Y. He, Chem. Commun. 54 (2018) 4947–4950.
[79] M. Dasog, G.B. De los Reyes, L.V. Titova, F.A. Hegmann, J.G.C. Veinot, ACS Nano 8 (2014) 9636–9648.
[80] J.A. Kelly, A.M. Shukaliak, M.D. Fleischauer, J.G.C. Veinot, J. Am. Chem. Soc. 133 (2011) 9564–9571.
[81] F. Sangghaleh, I. Sychugov, Z.Y. Yang, J.G.C. Veinot, J. Linnros, ACS Nano 9 (2015) 7097–7104.
[82] M. Dasog, Z.Y. Yang, S. Regli, T.M. Atkins, A. Faramus, M.P. Singh, et al., ACS Nano 7 (2013) 2676–2685.
[83] M. Dasog, K. Bader, J.G.C. Veinot, Chem. Mater. 27 (2015) 1153–1156.
[84] I.M.D. Hçhlein, A. Angi, R. Sinelnikov, J.G.C. Veinot, B. Rieger, Chem. Eur. J. 21 (2015) 2755–2758.
[85] K.Q. Peng, X. Wang, X.L. Wu, S.T. Lee, Nano Lett. 9 (2009) 3704–3709.
[86] K.Q. Peng, S.T. Lee, Adv. Mater. 23 (2011) 198–215.
[87] Z. Peng, H. Hu, M.I.B. Utama, L.M. Wong, K. Ghosh, R. Chen, et al., Nano Lett. 10 (2010) 3940–3947.
[88] Y. He, S. Su, T. Xu, Y. Zhong, J.A. Zapien, J. Li, et al., Nano Today 6 (2011) 122–130.
[89] Y. He, Y. Zhong, F. Peng, X. Wei, Y. Su, S. Su, et al., Angew. Chem. Int. Ed. 50 (2011) 3080–3083.
[90] F. Erogbogbo, K.T. Yong, R. Hu, W.C. Law, H. Ding, C.W. Chang, et al., ACS Nano 4 (2010) 5131–5138.
[91] H. Jiang, C.S. Chen, J. Phys. Chem. A 119 (2015) 3753–3761.
[92] K. Nomoto, H. Sugimoto, A. Breen, A.V. Ceguerra, T. Kanno, S.P. Ringer, et al., J. Phys. Chem. C 120 (2016) 17845–17852.

[93] B. Somogyi, R. Derian, I. Štich, A. Gali, J. Phys. Chem. C 121 (2017) 27741–27750.
[94] R. Limpens, M. Fujii, N.R. Neale, T. Gregorkiewicz, J. Phys. Chem. C 122 (2018) 6397–6404.
[95] T. Velusamy, S. Mitra, M.M. Montero, V. Svrcek, D. Mariotti, ACS Appl. Mater. Interfaces 7 (2015) 28207–28214.
[96] D.J. Rowe, J.S. Jeong, K.A. Mkhoyan, U.R. Kortshagen, Nano Lett. 13 (2013) 1317–1322.
[97] X. Zhang, M. Brynda, R.D. Britt, E.C. Carroll, D.S. Larsen, A.Y. Louie, et al., J. Am. Chem. Soc. 129 (2007) 10668–10669.
[98] C. Tu, X. Ma, P. Pantazis, S.M. Kauzlarich, A.Y. Louie, J. Am. Chem. Soc. 132 (2010) 2016–2023.
[99] M.P. Singh, T.M. Atkins, E. Muthuswamy, S. Kamali, C. Tu, A.Y. Louie, et al., ACS Nano 6 (2012) 5596–5604.
[100] K. Sato, S. Yokosuka, Y. Takigami, K. Hirakuri, K. Fujioka, Y. Manome, et al., J. Am. Chem. Soc. 133 (2011) 18626–18633.
[101] S. Zhou, Z. Ni, Y. Ding, M. Sugaya, X.D. Pi, T. Nozaki, ACS Photonics 3 (2016) 415–422.
[102] B.F.P. McVey, J. Butkus, J.E. Halpert, J.M. Hodgkiss, R.D. Tilley, J. Phys. Chem. Lett. 6 (2015) 1573–1576.
[103] S. Chandra, Y. Masuda, N. Shirahata, F.M. Winnik, Angew. Chem. Int. Ed. 56 (2017) 6157–6160.
[104] B.B. Chu, B. Song, X.Y. Ji, Y.Y. Su, H.Y. Wang, Y. He, Anal. Chem. 89 (2017) 12152–12159.
[105] B. Song, Y.L. Zhong, H.Y. Wang, Y.Y. Su, Y. He, Chem. Commun. 53 (2017) 6957–6960.
[106] B. Song, H.Y. Wang, Y.L. Zhong, B.B. Chu, Y.Y. Su, Y. He, Nanoscale 10 (2018) 1617–1621.
[107] J. Liu, F. Erogbogbo, K.T. Yong, L. Ye, J. Liu, R. Hu, et al., ACS Nano 7 (2013) 7303–7310.
[108] J.H. Park, L. Gu, G. Maltzahn, Ruoslahti E, S.N. Bhatia, M.J. Sailor, Nat. Mater. 8 (2009) 331–336.
[109] L. Gu, D.J. Hall, Z.T. Qin, E. Anglin, J. Joo, D.J. Mooney, et al., Nat. Commun. 4 (2013) 2326–2333.
[110] E. Phillips, O. Penate-Medina, P.B. Zanzonico, R.D. Carvajal, P. Möhan, Y.P. Ye, et al.,Sci. Trans. Med. 6 (2014), 260ra149.
[111] J.Y. Pang, Y.Y. Su, Y.L. Zong, F. Peng, B. Song, Y. He, Nano Res. 9 (2016) 3027–3037.
[112] M.A. Kotterman, D.V. Schaffer, Nat. Rev. Genet. 15 (2014) 445–451.
[113] C.Y. Tay, M.I. Setyawati, D.T. Leong, ACS Nano 11 (2017) 2764–2772.
[114] C. Zylberberg, K. Gaskill, S. Pasley, S. Matosevic, Gene Ther. 24 (2017) 441–452.
[115] H.P. Xu, Z.Y. Li, J. Si, J. Biomed. Nanotechnol. 10 (2014) 3483–3507.
[116] Z. Rehman, D. Hoekstra, I.S. Zuhorn, ACS Nano 7 (2013) 3767–3777.
[117] X.Y. Ji, C.Y. Wang, M.M. Tang, D.X. Guo, F. Peng, Y.L. Zhong, et al., Nanoscale 10 (2018) 14455–14463.
[118] Z.H. Liu, Y.Z. Li, W. Li, C. Xiao, D.F. Liu, C. Dong, et al.,Adv. Mater. 30 (2018), 1703393.
[119] V. Delplace, S. Payne, M. Shoichet, J. Control. Release 219 (2015) 652–668.
[120] R.C. Renaud, H. Xuereb, Nat. Rev. Drug Discovery 2 (2003) 425–426.
[121] N. Rama, A. Dubrac, T. Mathivet, R.A.N. Chárthaigh, G. Genet, B. Cristofaro, et al., Nat. Med. 21 (2015) 483–491.
[122] A. Chopdar, U. Chakravarthy, D. Verma, BMJ-Br. Med. J. 326 (2003) 485–488.
[123] M.M. Tang, X.Y. Ji, H. Xu, L. Zhang, A.R. Jiang, B. Song, et al., Anal. Chem. 90 (2018) 8188–8195.
[124] D. Tarn, C.E. Ashley, M. Xue, E.C. Carnes, J.I. Zink, C.J. Brinker, Acc. Chem. Res. 46 (2013) 792–801.
[125] M.I. Setyawati, D.T. Leong, ACS Appl. Mater. Inter. 9 (2017) 6690–6703.
[126] D.H. Jo, J.H. Kim, Y.S. Yu, T.G. Lee, J.H. Kim, Nanomed. Nanotechnol. 8 (2012) 784–791.
[127] C.X. Song, Y.L. Zhong, X.X. Jiang, F. Peng, Y.M. Lu, X.Y. Ji, et al., Anal. Chem. 87 (2015) 6718–6723.
[128] B.B. Chu, H.Y. Wang, B. Song, F. Peng, Y.Y. Su, Y. He, Anal. Chem. 88 (2016) 9235–9242.
[129] X.R. Li, X.C. Yang, Z.Q. Lin, D. Wang, D. Mei, B. He, et al., Eur. J. Pharm. Sci. 76 (2015) 95–101.
[130] K.C. Nitiss, J.L. Nitiss, Clin. Cancer Res. 20 (2014) 4737–4739.
[131] F. Cheung, Nature 480 (2011) S82–S83.
[132] R. Stone, Science 319 (2008) 709–710.
[133] L.K. Tsou, M.L. Tejero, J.R. Figura, Z.J. Zhang, Y.C. Wang, J.S. Yount, et al., J. Am. Chem. Soc. 138 (2016) 2209–2218.
[134] J. Mann, Nat. Rev. Cancer 2 (2002) 143–148.
[135] F.E. Koehn, G.T. Carter, Nat. Drug Discov. 4 (2005) 206–220.
[136] A.L. Harvey, Drug Discov. Today 13 (2008) 894–901.
[137] X.Y. Ji, D.X. Guo, B. Song, S.C. Wu, B.B. Chu, Y.Y. Su, et al., Nano Res. 11 (2018) 5629–5641.
[138] A. Jiang, B. Song, X. Ji, F. Peng, H. Wang, Y. Su, et al., Nano Res. 11 (2018) 2285–2294.
[139] F. Peng, M.I. Setyawati, J.K. Tee, X. Ding, J. Wang, M.E. Nga, et al., Nat. Nanotechnol. (2019), http://dx.doi.org/10.1038/s41565-018-0356-z.
[140] M.I. Setyawati, C.Y. Tay, B.H. Bay, D.T. Leong, ACS Nano 11 (2017) 5020–5030, 11.
[141] X. Ding, F. Peng, J. Zhou, W. Gong, G. Slaven, K.P. Loh, et al., Nat. Commun (2019), doi: 10.41.10.1038/s41467-018-07835-1.
[142] M.I. Setyawati, C.Y. Tay, S.L. Chia, S.L. Goh, W. Fang, M.J. Neo, Nat. Commun. 4 (2013) 1673–1685.
[143] J. Wang, L. Zhang, F. Peng, X. Shi, D.T. Leong, Chem. Mater. 30 (2018) 3759–3767.
[144] M.I. Setyawati, V.N. Mochalin, D.T. Leong, ACS Nano 10 (2016) 1170–1181.
[145] C.M.J. Hu, R.H. Fang, K.C. Wang, B.T. Luk, S. Thamphiwatana, D. Dehaini, et al., Nature 526 (2015) 118–121.
[146] J.M.A. Blair, M.A. Webber, A.J. Baylay, D.O. Ogbolu, L.J.V. Piddock, Nat. Rev. Microbiol. 13 (2015) 42–51.
[147] A. Trampuz, W. Zimmerli, Injury 37 (2006) S59–S66.
[148] M.E. Brecher, S.N. Hay, Clin. Microbiol. Rev. 18 (2005) 195–204.
[149] S.B. Levy, B. Marshall, Nat. Med. 10 (2004) S122–S129.
[150] E.J. Kwon, M. Skalak, A. Bertucci, G. Braun, F. Ricci, E. Ruoslahti, et al.,Adv. Mater. 29 (2017), 1701527.
[151] X. Zhai, B. Song, B.B. Chu, Y.Y. Su, H.Y. Wang, Y. He, Nano Res. 11 (2018) 6417–6427.
[152] G. Hong, A.L. Antaris, H. Dai, Nat. Biomed. Eng. 1 (2017), 0010.
[153] K.R. Bhushan, P. Misra, F. Liu, S. Mathur, R.E. Lenkinski, J.V. Frangioni, et al., J. Am. Chem. Soc. 130 (2008) 17648–17649.
[154] K. Welsher, S.P. Sherlock, H. Dai, Proc. Natl. Acad. Sci. U.S.A. 108 (2011) 8943–8948.
[155] D. Kim, J. Kang, T. Wang, H.G. Ryu, J.M. Zuidema, J. Joo, et al.,Adv. Mater. 29 (2017), 1703309.
[156] F. Patolsky, B.P. Timko, G. Yu, Y. Fang, A.B. Greytak, G. Zhengr, et al., Science 313 (2006) 1100–1104.
[157] A. Zhang, C.M. Lieber, Chem. Rev. 116 (2016) 215–257.
[158] X. Dai, G. Hong, T. Gao, C.M. Lieber, Acc. Chem. Res. 51 (2018) 309–318.
[159] T.M. Fua, G. Honga, R.D. Viverosb, T. Zhoua, C.M. Liebera, Proc. Natl. Acad. Sci. U. S. A. 114 (2017) 10046–10055.
[160] G. Hong, T.M. Fu, M. Qiao, R.D. Viveros, X. Yang, T. Zhou, et al., Science 360 (2018) 1447–1451.

Bin Song received his bachelor degree (2013) in chemistry from Jiangsu Normal University (China), and continued the graduate study (Master and Doctor) in Soochow University (China) in 2013–2019. He is currently a Ph.D. student under the supervision of Prof. Yao He in Institute of Functional Nano & Soft Materials (FUNSOM) at Soochow University (China). His research interest focuses on the development of functional silicon nanomaterials for various optical applications (e.g., sensing, bioimaging, cancer therapy, light-emitting diodes, and laser).

Yao He received his bachelor and Ph.D degree from Fudan University (China), and then continued his further research as postdoctor or visiting scholar in Shanghai Institute of Applied Physics (Chinese Academy of Sciences, China), City University of Hong Kong (China), and Stanford University (U.S). He is now the Principal Investigator of Institute of Functional Nano & Soft Materials (FUNSOM) at Soochow University in China. Starting from 2009 when Dr. He established his group, he has authored over 100 peer-reviewed papers, with SCI citation number of ~7000. Currently, he is the Associate Editor (2017-) of Frontiers in Chemistry (nanoscience section). He served as a chief scientist of the "youth 973" project (National key scientific research projects) in 2013. Dr. He received the awards including the National Science and Technology Leading Talent Award in 2012, the First Prize of Jiangsu Science and Technology Award in 2017 (Ranking first), and NFSC Distinguished Young Scholar Award in 2018.